THESIS FOR THE DEGREE OF DOCTOR OF PHILOSOPHY

in

Thermo and Fluid Dynamics

THE EFFECTS OF VARIOUS NOZZLE HOLE CONFIGURATIONS ON DIESEL ENGINE PERFORMANCE

by

ANDREAS MATSSON

Department of Applied Mechanics
CHALMERS UNIVERSITY OF TECHNOLOGY
Göteborg, Sweden, 2013

THE EFFECTS OF VARIOUS NOZZLE HOLE CONFIGURATIONS ON DIESEL ENGINE PERFORMANCE

ANDREAS MATSSON
ISBN 978-91-7385-953-0

Doktorsavhandling vid Chalmers tekniska högskola
Ny serie nr 3635
ISSN: 0346-718X

Department of Applied Mechanics
Chalmers University of Technology
SE-412 96 Göteborg
Sweden
Telephone +46 (0)31 7721000

Abstract

Any improvement that can be done with the diesel engine to reduce emissions and fuel consumption is of importance. The aim of the studies presented in this thesis was to determine whether changes in the nozzle geometry of the fuel injection systems used in diesel engines might improve their emissions and fuel consumption. This project started with the question if elliptical or non-circular nozzle holes instead of the conventional circular designs would have any effect on emissions and fuel consumption in a heavy duty diesel engine. It was speculated that non-circular holes might increase air entrainment in the lift-off zone and thereby reduce smoke emissions. Increased air entrainment in the lift off zone would allow more of the fuel to burn under relatively lean conditions in the rich premixed zone and thus reduce soot formation. Experiments were conducted using a single cylinder engine whose emissions and fuel consumption were measured. An optical cylinder head was also designed and manufactured, and used to investigate flame propagation during combustion using fuel injectors with non-circular nozzles.

The effects of varying the nozzle hole inlet geometry were also investigated by conducting experiments with single-hole axisymmetric nozzles that had been subjected to different grades of hydrogrinding. These studies were performed using a high temperature high pressure combustion chamber, and a variety of techniques were used to characterise the resulting sprays and flames. Impingement measurements were also performed to ensure that the studied nozzles produced fuel jets with the same momentum. From the impingement measurements velocity, discharge coefficient and loss of kinetic energy was calculated.

Finally, the effects of changing the nozzle hole inlet geometry were investigated using a single cylinder heavy duty diesel engine. The engine's emissions and fuel consumption were measured and an endoscope technique was used to capture images from inside the combustion chamber during the combustion sequence. Two-colour pyrometry was used to determine the soot and temperature distributions inside the cylinder from the images, and the results of this analysis were compared to the emissions data.

Acknowledgements

This thesis could have been finished more than 11 years ago if it wasn't for an accident with subsequent major consequences. During many extremely difficulty years I was convinced that it would never be completed, but thanks to Jenny "Lakritz" Magnusson who help me and also raised our two fantastic boys Oscar and Hampus I was able to recover. Thank you Jenny! Also, thank you Oscar and Hampus for being the best of friends!

Mum and dad, Clary and Ulf, have also given great support during the years and still are. Thank you both! Mum sometimes said to me when I was a kid, that whatever I did I should get an education and now it feels like I have.

Henrik Landälv and Sören Udd at former Volvo Lastvagnar, made it possible for me to start the PhD education. The work has been financed by CERC – Combustion Engine Research Center where Volvo AB, among other companies, and also Swedish National Energy Administration have supported financially. Thank you for the support and giving me the opportunity.

At Chalmers it has been many long days, but thanks to all cheerful PhD colleagues and staff works was easier, with many fun lunches, "after works" and "Institution days".

At the start of the project Jerzy Chomiak was my professor but he was later replaced by Ingemar Denbratt. Thank you both for your support and giving me a second chance.

Thank you, Sven Andersson, for being my supervisor with a smile and for taking extra care of the report details and giving me a second chance.

A special thank you to Savo Girja who has helped me with countless hours of engine testing. Thank you to all to the staff in the mechanical work shop.

Thank you for administrative support Sandra, Ulla and Elinor.

I'd like to thank my roommates Lionel Ganippa and Pär Bergstrand for numerous discussions around diesel engine and sprays. An extra thank you to Lionel with whom I collaborated together doing experiments and writing an article from these results. I'd also like to thank all other PhD student colleagues for the fun time…there are too many to mention any.

Publications included in this thesis

1. **The Effect of Elliptical Nozzle Holes on Combustion and Emission Formation in a Heavy Duty Diesel Engine, SAE 2000-01-1251,**

   Andreas Matsson
   Volvo Truck Corporation and Chalmers University of Technology, Gothenburg, Sweden

   Lisa Jacobsson, Sven Andersson
   Chalmers University of Technology, Gothenburg, Sweden

2. **The effect of nozzle inlet conditions on fuel consumption and emissions of a heavy duty diesel engine, JSAE 2001-5345**

   Andreas Matsson
   Volvo Truck Corporation and Chalmers University of Technology, Gothenburg, Sweden

3. **The Effect of Non-Circular Nozzle Holes on Combustion and Emission Formation in a Heavy Duty Diesel Engine, SAE 2002-01-2671**

   Andreas Matsson
   Volvo Truck Corporation and Chalmers University of Technology, Gothenburg, Sweden

   Sven Andersson
   Department of Thermo and Fluid Dynamic, Chalmers University of Technology, Gothenburg, Sweden

4. **Combustion Characteristics of Diesel Sprays From Equivalent Nozzles With Sharp And Rounded Inlet Geometries. Combustion Science and Technology, 176 (6), 1015-1032. 2003.**

   Lionel Christopher Ganippa, Sven Andersson and Jerzy Chomiak
   Department of Thermo and Fluid Dynamics, Chalmers University of Technology, Gothenburg, Sweden

   Andreas Matsson
   Volvo Powertrain, and Chalmers University of Technology, Gothenburg, Sweden

5. **Comparing Different Grades of Hydro Grinded Nozzles in a Heavy Duty Diesel Engine, SAE 2003-01-3420**

   Andreas Matsson,
   Volvo Powertrain and Chalmers University of Technology, Gothenburg, Sweden

   Savo Gjirja, Sven Andersson
   Department of Thermo and Fluid Dynamic, Chalmers University of Technology, Gothenburg, Sweden

Author’s contributions to papers 1 - 5.

Paper 1.

Planned and analysed the experiments, assisted in operating the engine, and was the main author of the paper.

Paper 2.

Planned and analysed the experiments, assisted in operating the engine, and was the main author of the paper.

Paper 3.

Planned, analysed, and set up the experiments, assisted in operating the engine, and was the main author of the paper. Designed and manufactured an optical cylinder head. The author conceived all of the ideas and conducted the design work but did not create the CAD drawings or cam profile. Residual gas calculations were performed at Volvo Group Truck Technology.

Paper 4.

Planned, set up, ran and analysed the experiments together with main-author. Co-wrote the paper.

Paper 5.

Planned, evaluated, and set up the experiments, assisted in operating the engine, and was the main author of the paper.

Publications from the project that are not included in this thesis:

1. **Particles from Diesel engine combustion – A review, Internal report 003, 2000, Thermo and Fluid Dynamic, Chalmers, Sweden**

   Andreas Matsson,
   Volvo Truck Corporation and Chalmers University of Technology, Gothenburg, Sweden

2. **Combination of methods for characterization diesel engine exhaust particulate emissions**. JSME International Journal, Series B: Fluids and Thermal Engineering. 2001;44(1):166-170.

   Moh'd Abo-Qudais
   Mech. Eng. Dept. Jordan University of Science and Technology

   Andreas Matsson
   Volvo Truck Corporation and Chalmers University of Technology, Gothenburg, Sweden

   David Kittelson
   Mech. Eng. Dept. University of Minnesota

Abbreviations

NO_x	Nitrogen Oxides
NO	Nitrogen monoxide
NO_2	Nitrogen dioxide
PM	Particulate Matter
C	Carbon
CO	Carbonmonoxide
CO_2	Carbon Dioxide
OH	Hydroxide
NH	Nitrogen monohydride
HCN	Hydrogen cyanide
H_2CN	Dihydrogen cyanide
CN-	Cyano radical
HC	Hydro Carbons
BSFC	Brake Specific Fuel Consumption
mm	millimeter
µm	micrometer
µs	microsecond
nm	nanometer
L	Litre
SI	Spark Ignited
DI	Direct Injected
EC	European Community
ECE R-49	Economic Commission for Europe - Regulation No 49
m/s	meters per second
TDC	Top Dead Center
CN	Cavitation Number
Re	Reynolds number
We	Weber number
K-factor	Conicity
D	diameter
d	diameter
PIV	Particle Image Velocimetry
v_{max}	maximum injection velocity
v_{mean}	average velocity
Δp	pressure drop over the nozzle hole
ρ_{fuel}	fuel density
ρ_a	air density
c_d	discharge coefficient
µ	discharge coefficient (used in figure 12)
v_c	corrected injection velocity
c_v	velocity correction factor
c_a	area correction factor
$A_{effective}$	effective area
$A_{geometrical}$	geometrical area
$\dot{m}$	mass flow
s	spray tip penetration

t	time
CR	Common Rail
PLD	Pumpe Leitung Düse (German) – Pump Line Nozzle
SMD	Sauter Mean Diameter
HG	Hydro Grinding
ASI	After Start of Injection
PAH	Poly Aromatic Hydrocarbons
K	Kelvin degree
T	Temperature
Θ	Spray angle
ξ_{St}	percentage of stoichiometry
ϕ	fuel/air ratio
AVL	Anstalt für Verbrennungskraftmaschinen List
EUI	Electronic Unit Injector
CAD	Computer Aided Design or Crank Angle Degree
SAE	Standard Automotive Engineering
EGR	Exhaust Gas Recirculation
CCD	Charge Coupled Device
RoHR	Rate of Heat Release
REF	Reference
SOI	Start of Injection
EOI	End of Injection
AR	Aspect Ratio

Table of contents

1. Introduction
2. Objectives
3. The Diesel engine – how it all began
4. Diesel engine fuel conversion efficiency
5. Emissions regulations
6. Diesel engine combustion
    - 6.1 General introduction
    - 6.2 Fuel injection system
    - 6.3 Cavitation
    - 6.4 Nozzle flow experiments
        - 6.4.1 Nozzle flow studies using upscaled nozzles
        - 6.4.2 Nozzle flow through real size single hole nozzles
        - 6.4.3 Nozzle flow with real size multi hole nozzles
        - 6.4.4 Nozzle damage due to cavitation
        - 6.4.5. String cavitation
    - 6.5 The discharge coefficient
    - 6.6 The discharge coefficient as a function of the inlet radius
7. Diesel spray formation
    - 7.1 Spray formation – atomization
    - 7.2 Spray characteristics
        - 7.2.1 Break up length
        - 7.2.2 Liquid length
        - 7.2.3 Spray cone angle
        - 7.2.4 Drop size
    - 7.3 The effect of hydrogrinding/hydro erosion on injection velocity
8. Combustion and emission formation in diesel sprays
    - 8.1 Introduction
    - 8.2 Dec's conceptual model
    - 8.3 Air entrainment
    - 8.4 Wall impingement
    - 8.5 Soot formation
    - 8.6 Soot particles
    - 8.7 Engine out soot emissions
    - 8.8 NO_x formation

8.9 The particle - NO_x trade off
9. Engine experimental equipment
9.1 The engine
9.2 Engine optical studies
9.3 Endoscope
10. Experimental equipment used for spray studies
11. Summary of results
12. Conclusions
13. References

1. Introduction

The diesel engine has the highest fuel conversion efficiency of the various internal combustion engines and also normally has a long operational lifetime. It is therefore widely used in diverse applications and is the dominant engine type in ships and trucks due to its superior overall economic performance. Diesel engines are also becoming increasingly important power sources for lighter vehicles such as passenger cars due to their increased power output, low noise levels, and the ongoing rise in fuel prices. The diesel engine is thus arguably the most important energy converter in modern transportation systems.

The drawbacks of the diesel engine relate to its emissions profile, which is dominated by nitrogen oxides, NO_x and particulate matter (PM). NO_x causes eye, throat and lung irritation and contributes to the formation of photochemical smog, ground level ozone and acid rain. Particulate matter has adverse effects on human health, reduces visibility, and soils buildings. It is believed that particles with a diameter of less than 2.5 μm have particularly severe effects on human health, and diesel engines emit a relatively large amount of particles in this size range. Finally, the combustion of diesel fuel generates carbondioxide. Since carbon dioxide is a greenhouse gas and is believed to be an important cause of global climate change, its emissions should be minimized. The main raw material used to make diesel fuel is crude oil. Conventional diesel is often blended with non-fossil fuels such as methyl esters derived from sources such as rapeseed oil, soybean oil, palm oil or pine tree oil, but EC regulations state that the proportion of these oils in the final fuel may not exceed 5.75 %. Crude oil is a finite resource, and it was estimated that the known oil reserves in 2011 would be exhausted within around 50 years [1]. Natural gas and coal can also be converted into a fuel with properties similar to those of diesel, but this is still a limited fossil fuel whose combustion will contribute to the greenhouse effect. Because of all these factors, there is a need to reduce the emissions and fuel consumption of modern diesel engines.

2. Objectives

The initial aim of the project presented in this thesis was to answer the following question: How are the emissions and fuel consumption of heavy duty diesel engines affected by replacing the circular nozzle holes of their fuel injectors with elliptical or other non-circular holes? It has been observed that gas jets emitted through non-circular holes exhibit a higher level of air entrainment than those emitted through conventional circular holes. In some cases, the use of non-circular nozzle holes causes a phenomenon known as axis-switching, in which the jet spreading angle in the minor axis plane exceeds that in the major axis plane. Axis switching has also been observed in sprays emitted from elliptical holes when a liquid was injected into a gas. Increasing the degree of air entrainment in the lift-off zone of a diesel fuel jet might reasonably be expected to reduce the amount of soot formation. To evaluate this hypothesis, experiments were conducted in which the emissions and fuel consumption of a single cylinder engine were measured. An optical cylinder head was also designed and manufactured for use in tests of flame propagation in sprays formed using non-circular nozzles.

A second objective was to determine how the grade of hydrogrinding applied to the nozzle hole affected spray and flame formation and the engine's emissions and fuel consumption.

Hydrogrinding is used in manufacturing to create a radius on nozzle inlets. The presence of a radius reduces cavitation damage to the nozzle hole and increases the stability of the volume flow during engine operation. Experiments on the effects of hydrogrinding were conducted in a high temperature high pressure combustion chamber. A range of single-hole axisymmetric nozzles with different grades of hydrogrinding were tested, and the sprays and flames produced in each case were characterized using various experimental techniques. Impingement measurements were conducted to ensure that both of the selected nozzles produced jets with the same momentum for a given pressure drop. The impingement measurements were then used to determine the velocity, discharge coefficient and loss of kinetic energy for the spray.

The effects of varying the nozzle hole inlet geometry were also investigated using a single cylinder heavy duty diesel engine. The engine's emissions and fuel consumption were measured and an endoscope was used to capture images during the combustion sequence. The

endoscope images were analyzed by means of two-colour pyrometry in order to determine the soot concentrations and flame temperature, and the results of these analyses were compared to the emissions measurements.

3. The Diesel engine – how it all began

The Diesel engine is named from Rudolf Diesel, who was born in Paris in 1858 and filed a patent named "Arbeitsverfahren und Ausführungsart für Verbrennungsmaschinen" in 1892. The patent was granted on the 23rd of Febuary 1893 in Germany, and assigned the patent number DRP 67 207. Rudolf Diesel had studied engineering and, drawing inspiration from the thermodynamic Carnot process, aimed to make an internal combustion engine that would have greater thermodynamic and mechanical efficiencies than those of the steam and Otto engines of the time, which were around 10%. Diesel's first engine was ignited for the first time on the 10th of August, 1893, in Augsburg, Germany. It was a ten foot tall single cylinder engine with a swept volume of 7 litres, using a fuel that resembled petrol and may have been Ligroin. Unlike the Otto engine, it used the heat of the compressed air to ignite the fuel rather than relying on an igniter. Ligroin was the fuel used in the first automobile, the Benz Patent-Motorwagen Nummer 3, which had an Otto engine.

Several other inventors were working on engines that resembled Diesel's design during this era. In 1886, at 24 years of age, Herbert Akroyd Stuart built a prototype compression ignition engine that ran on paraffin (lamp oil), which is still regarded as a good fuel for diesel engines today. Together with Charles Richard Binney, he filed patent No 7146 in May 1890, with the title "Improvements in Engines Operated by the Explosion of Mixtures of Combustible Vapor or Gas and Air". They started building engines based on this patent on the 26th of June, 1891 and sold them commercially starting from the 8th of July, 1892. The difference between Stuart's and Diesel's designs was that Diesel used a higher degree of compression, with the fuel being vaporized and ignited by the hot air. Conversely, Stuart used a low compression engine with a pre-chamber containing a hot surface into which the fuel was injected. This surface needed to be heated to start the engine.

When Diesel ran his first engine in 1893, it ignited but did not run steadily. The development of improved piston rings and an air-assisted fuel injection system enabled the engine to run by itself for a minute on the 17th of February 1894, using a petrol-like fuel. Diesel continued to refine the engine, experimenting with the use of pre-chambers and pre-vaporization and in June 1895, he introduced a new design with a swept volume of 15.2 L that achieved a mechanical efficiency of 17% and 14 hk at 88 rpm. He presented another new design in 1896

that incorporated some of his original ideas, including direct fuel injection and air-assisted fuel injection. However, this engine also featured a water-cooled piston, which proved to be a key breakthrough. His new 19.6 L engine achieved a mechanical efficiency of 30.2 % in October 1897 and was rapidly commercialized [2]. Because Stuart's engines used low compression ratios, they could not match the thermal efficiency of Diesel's; within a few decades, Stuart was out of business.

4. Diesel engine fuel conversion efficiency

The efficiency of the Diesel engine depends on the engine's size, ranging from around 40 % for a small-bore high speed engine for passenger cars to around 45 % for heavy duty engines and slightly above 50 % for the large-bore low speed engines used in marine applications. The engine's efficiency increases as the speed decreases because lower speeds mean less energy lost to friction. Low speed engines also normally have comparatively low area/volume ratios, which are beneficial in terms of heat loss.

Diesel engines are more efficient than premixed spark-ignited (SI) engines for several reasons. Specifically, compared to SI engines, diesel engines have:

- **Higher compression ratios** - The high compression ratios of diesel engines mean they have high expansion ratios and so the temperature and pressure drop as the gas expands in the cylinder is greater than that achieved in a comparable SI engine.
- **Higher air excess ratios** - The higher air excess ratio decreases the exhaust temperature, thereby reducing exhaust and cooling losses.
- **Higher heat capacity ratios** - The diesel engine compresses pure air which has a higher heat capacity ratio, about 1.4, than the air-fuel mixture used in SI engines, for which the heat capacity ratio is around 1.3. The heat capacity ratio of the in-cylinder gas during the expansion stroke is also higher in a diesel engine. Therefore, for a given volume-expansion ratio, the burned gases in a diesel engine expand over a greater temperature range before being exhausted than they do in an SI engine, and the expansion stroke work done per unit mass of fuel is increased.
- **Unthrottled intakes** - Diesel engines operate without throttling, which reduces pumping losses, especially at low loads.

5. Emissions regulations

The world's first law regulating emissions was passed in 1580, when Queen Elizabeth of England prohibited the use of coal in London while Parliament was in session. The ban was passed due to concerns that the "health of the Knights of the Shires might suffer during their abode in the Metropolis." [3]. The first major air pollution problems caused by vehicles were the smogs that formed in Los Angeles, USA, in the 1940s; California introduced its first automobile emissions standards in the early 1960s [4]. The first exhaust emission regulations for the heavy duty diesel-engined vehicles were passed in the USA in 1986. Until then, diesel engines had been considered 'clean', with low levels of carbon monoxide and hydrocarbon emissions relative to spark ignition (SI) engines. However, over the last 25 years, legislators have become increasingly concerned with exhaust emissions and engine noise. As shown in figure 1, the permissible emissions of particulate matter (PM) and NO_x from heavy duty engines have been reduced by a factor of 20 over the last 20 years [5]. The Euro 6 standards that will be introduced as incentive in 2013 and a mandatory requirement in 2014 will impose restrictions on both the mass of PM emitted and the number of individual particles that may be emitted.

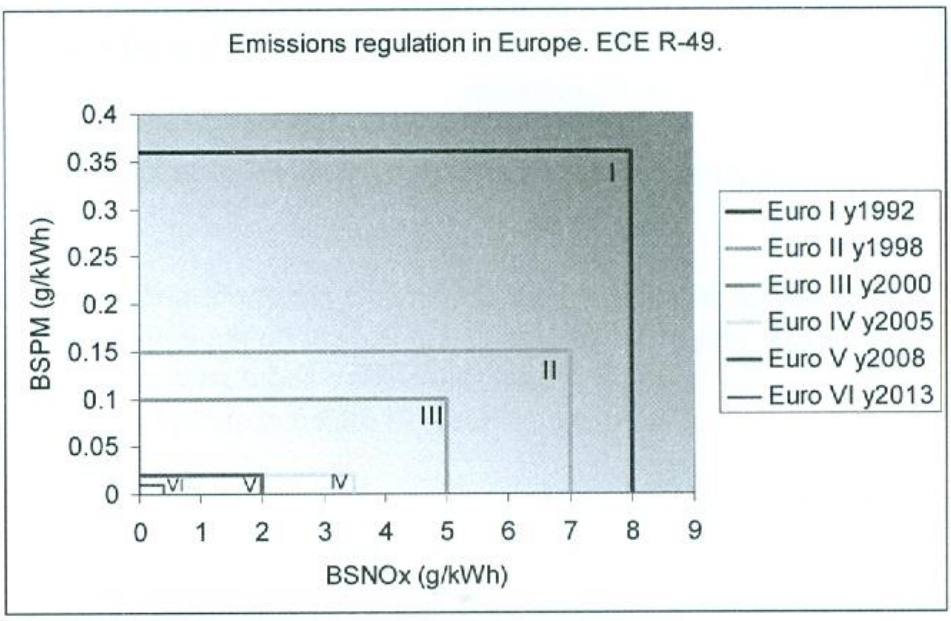

Figure 1. European emission regulations: the increasingly strict PM and NO_x emissions thresholds specified in the ECE R-49 standards for heavy duty road vehicles [5].

Due to the progressive decrease in the emissions output of modern vehicles and the growing concerns over global warming and fuel prices, there has been an increasing emphasis on reducing engines' CO_2 emission and thus their fuel consumption. The need to achieve the desired low emission levels development of technical solution of the engine itself has been extensive, but also on exhaust gas after treatment systems.

The most problematic regulated emissions from diesel engines are nitrogen oxides (NO_x) and particulate matter (PM). NO is rapidly oxidised to NO_2, which causes eye, throat and lung irritation. NO_2 also forms photochemical smogs, ground level ozone, acid rain, nutrient overloading in bodies of water, and destroys ozone in the stratosphere. Particulate matter emissions are concerning because they can have adverse effects on human health, reduce visibility, and soil buildings. Other emissions from diesel engines include carbon monoxide (CO), unburned hydrocarbons (HC), carbon dioxide (CO_2) and noise. Carbon monoxide reduces the oxygen-carrying capacity of the blood by reacting with haemoglobin, thereby depriving tissues of oxygen. Unburned hydrocarbons produce photochemical smog and promote ozone formation at ground level. In addition, some (e.g. the aromatics) are known to be carcinogenic. Excess air is always present during combustion in a diesel engine, so their emissions of CO and HC are always low. It is therefore relatively easy for diesel engines to meet emissions targets for these pollutants. Carbon dioxide has been identified as a greenhouse gas that is believed to cause global warming. Because almost all fuel that is used is based from crude oil, the level of carbon dioxide will increase. There are regulations for noise levels and improvements have been done through the years with combustion strategies, engine structure designs, insulation and improved muffler construction through computer calculations.

6. Diesel engine combustion

6.1 General introduction

In a diesel engine, air is trapped in a cylinder and compressed by a reciprocal piston, which increases its temperature and pressure. The fuel is pressurized in a pump and injected into the cylinder via nozzle holes, forming sprays of liquid that are rapidly atomized and vaporized. The injection velocity is typically on the order of 200 to 700 m/s, depending on the pressure difference between the nozzle sac and the compressed air. Fuel injection normally occurs when the piston is close to its upper position, which is known as the top dead center (TDC). At TDC, the pressure and temperature of the air are on the order of 100 bar and 600 °C, respectively. Ignition is initiated shortly after injection by the high temperature of the air in zones containing combustible mixtures. Figure 2 shows the nozzle housing, piston bowl and three parameters that are used to describe the properties of the fuel spray. Fuel that has mixed with air to form a combustible mixture will react quickly after ignition and burn in a premixed flame. A visible flame propagates quickly around the spray periphery, and the remaining fuel burns in a diffusion flame. When the injection stops, there is a burning cloud of fuel that is moving away from the nozzle. The design of the piston bowl is important for the combustion process because the burning cloud will strike the wall and its subsequent trajectory and behavior will be determined by the wall's properties. The bowl also controls the movement of gas within the cylinder, including the transportation of the fresh air that is required for the oxidation of the fuel. The volume enclosed by the boundaries of the piston, cylinder and cylinder head is called the combustion chamber. The complete oxidation of fuel in air produces water and CO_2. However, some fraction of the fuel will not undergo complete combustion, resulting in the formation of particulate matter, CO and HC. The majority of the engine's NO_x emissions form in localized regions of high temperature where air is present.

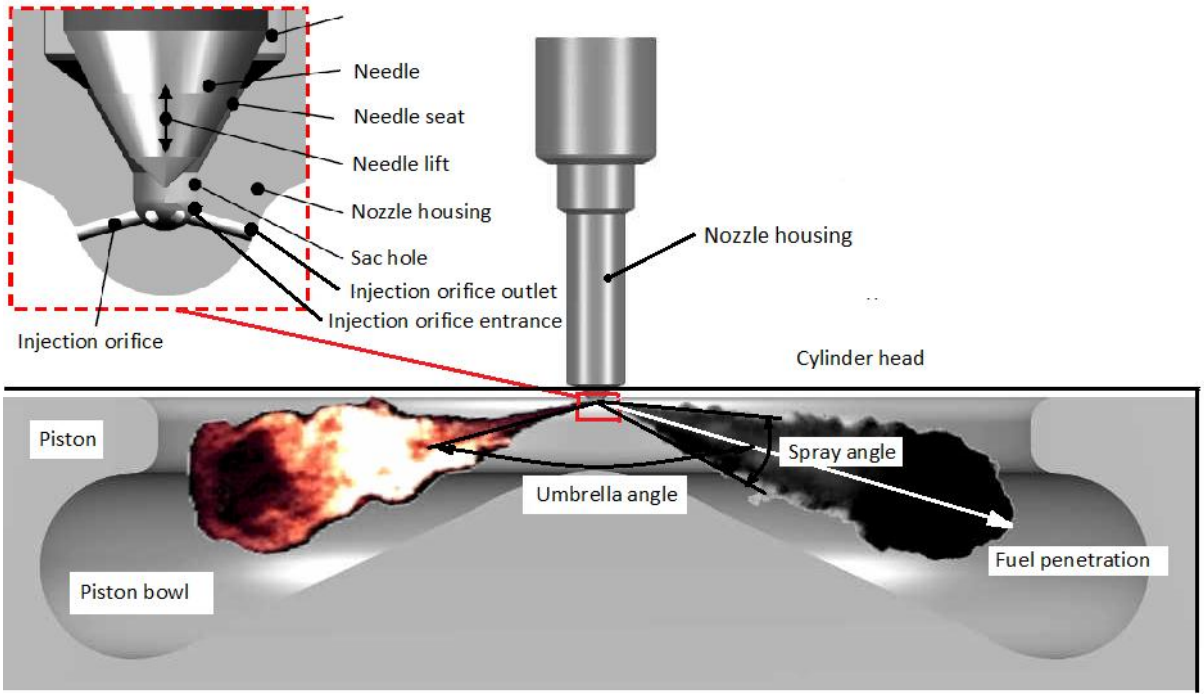

Figure 2. Nozzle housing, piston bowl and three parameters that are used to describe the properties of the fuel spray. Adapted from reference [6].

6.2 Fuel injection system

In brief, the most important parts of a diesel engine's fuel injection system are the pump, the control valve, and the nozzle body with its needle. The pump ensures that the fuel is sufficiently pressurized and the needle seals of the pressurized fuel from the combustion chamber. The needle is operated by adjusting the pressure differential between the needle top and bottom ends by utilizing a small electrically actuated control valve mounted above the needle. The needle starts to move once the difference between the hydraulic forces over the needle exceeds the spring load on the needle. As the needle moves, its lower conical area separates from the sealing seat, allowing fuel to enter the sac and nozzle hole. The fuel is typically discharged from the nozzle via 4–10 uniform holes at the tip, each with a diameter of 0.15-0.25 mm. The fuel mass flow is a function of the fuel density, the pressure difference between the nozzle sac and combustion chamber, and the total hydraulic area of the nozzle holes. The pressure inside the nozzle sac can be as high as 3000 bar and the maximum cylinder pressure in a modern diesel engine is in the order of 200 bar, so difference between the nozzle sac and combustion chamber pressures is large. Because the nozzle is typically around 1 mm long, the fuel experiences strong acceleration and can achieve injection

velocities of 700 m/s or more at the orifice exit. When the nozzle hole is manufactured, the edges of the inlet are sharp. A radius is created to soften the edge by grinding with an abrasive fluid (hydro erosion) or paste (hydro grinding). If a nozzle with a sharp inlet were used in an engine, the injected fuel would erode the sharp nozzle edges over time, causing the fuel flow to increase and thus changing the engine's power, torque and emissions.

6.3 Cavitation

It is difficult to investigate the conditions in the nozzle tip due to its small size and opacity, as well as the high fuel pressure and the forces that act on it during engine operation. The large pressure drop between the sac and the cylinder accelerates the fuel to high velocities over a very short distance. Fuel injection occurs over a very short period of time – on the order of a few milliseconds – and involves many transient flow phenomena. One of these phenomena that has been studied in some detail is cavitation. Cavitation occurs when the static pressure is lower than the vapour pressure of the fuel. Under such conditions, the fuel will undergo a phase transition, from the liquid to the vapour phase. The static pressure is low in some areas of the nozzle where there are large differences in velocity gradients, typically at the upper part of the hole entrance. The onset and degree of cavitation can be represented using a dimensionless parameter called the cavitation number (CN). The CN has been defined in many different ways, but they all relate to the ratio between a cavitation-forming and a cavitation-suppressing term. One widely used definition holds that the CN is a function of the upstream, downstream, and vapor pressures [7].

$$CN = \frac{P_{Upstream} - P_{Downstream}}{P_{Downstream} - P_{Vapour}}$$

- $P_{Upstream}$ - the upstream pressure, i.e. the injection pressure in the sac.
- $P_{Downstream}$ - the downstream pressure, i.e. the pressure of the gas in the cylinder.
- P_{Vapour} - the fuel's vapour pressure, which depends on the temperature and the fuel.

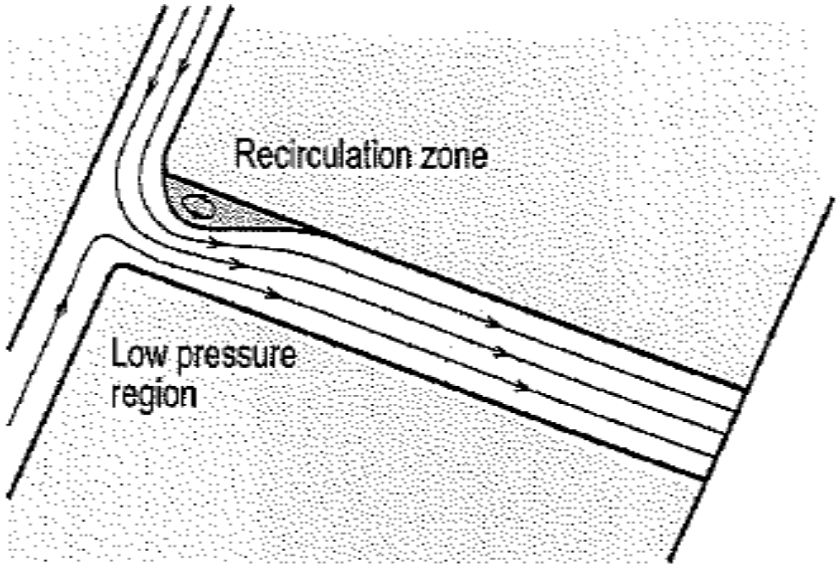

Figure 3. The recirculation zone at the nozzle hole inlet [8].

In sharp-edged nozzles, flow separation occurs in the region immediately downstream of the nozzle inlet. This creates a recirculation zone as shown in figure 3, along with a region of free flow where the fuel attains its maximum velocity. The flow separation occurs because of the fluid's inertia, which prevents it from flowing smoothly around the sharp corner. Consequently, the boundary layer separates and a cavity of fuel vapour may form if the pressure is low enough. Further downstream, the flow reattaches to the walls of the nozzle and the static pressure exceeds the vapor pressure, causing the cavitation bubbles to collapse. If the bubble were to exit the nozzle via the hole, it would have to collapse because the ambient pressure is greater than the fuel's vapor pressure [21]. Surface roughness has been identified as a trigger for cavitation [75] and small imperfections in the nozzle inlet provide favourable conditions for it to occur [21], but if the nozzle inlet radius is increased or the hole is shaped to provide a less sharp edge in the direction of the flow, the size of the recirculation zone and the nozzle's sensitivity to cavitation can be reduced [8]. Cavitation has a strong effect on nozzle flow performance because it reduces the discharge coefficient. In addition, while the atomisation process is not fully understood, it has been suggested that cavitation contributes to the fuel break-up process and subsequent atomisation [9]. Reitz and Bracco concluded that cavitation is not necessary for jet atomization but does have an effect [10]. Cavitation in the flow and the recirculation zone give the fuel a non-uniform velocity and density profile at the orifice exit. The rates of cavity formation and implosion fluctuate strongly the fuel injection phase. The cavities grow and collapse and also break away from their original positions in

clouds of cavitation bubbles that are transported downstream in a process known as shedding, which increases the irregularity of the spray formed from the injected fuel. The changes in the distribution of the vapor in the nozzle fuel flow have strong effects on its velocity profile [8]. These fluctuations also generate turbulence that is suggested to facilitate the disintegration of liquid jet [11,12] and has been suggested to be more important for atomization than cavitation itself [13]. Badock *et al.* identified the interaction between cavitation and turbulence as the most important parameter governing the initial spectrum of perturbation on the surface of the free jet (and therefore the primary breakup process), but found it difficult to separate the individual effects of turbulence and cavitation. [14].

6.4 Nozzle flow experiments

6.4.1 Nozzle flow studies using upscaled nozzles

Scaled-up models made from transparent materials have been used extensively to study the flow of fuel inside nozzles. Some investigations have also been conducted using normal-sized transparent nozzles, but scaled-up models have been more widely used to investigate the flow structure inside the nozzle tip. These studies are often performed using conditions that are less severe than those found in real engines, with comparatively low pressures and velocities [11,13,15,16,17]. Some experiments link the results from internal flow to the spray characteristics, and Ganippa [17] studied a single hole inclined nozzle and observed differences in spray structure together with the appearance of cavitation. Observations of a bushier spray and an increased spray angle on the same side as where the cavitation occurred were reported.

6.4.2 Nozzle flow through real -size single hole nozzles

The use of up-scaled nozzles causes issues with scaling effects. Compared to real-sized nozzles, scaled-up nozzles typically have different fluid velocities and produce larger bubbles that have different collapse times. Therefore, many authors have investigated real-sized nozzles with single holes. When considering nozzles with vertical axisymmetric holes, phenomena that are observed in single-hole nozzles are not always observed in their multi-hole counterparts, and vice-versa. A flow into a single vertical hole creates a symmetrical

velocity profile in the vicinity of the nozzle exit, with a higher fluid velocity than would be achieved in a multi hole nozzle that had a non-symmetrical velocity profile and the same hole shape [18]. With a single-hole nozzle and a needle, mainly film cavitation have been observed, a process in which a layer of cavitation is formed along the hole's periphery. In one notable study using a nozzle of this type, the entire ring surrounding the inlet was filled with bubbles within 20 microseconds following the opening of the valve, demonstrating that cavitation can occur over very short periods of time [19]. Even when using transparent nozzles with a size large enough to be used in truck engines (i.e. with diameters of less than 250 µm) the scope for optical access can be limited by the occurrence of cavitation. For example, shadowgraph studies are difficult to perform in such cases because of the total reflection of the cavitation film [20,21]. Blessing [6] investigated the effects of conicity and hydro erosion in transparent real size nozzles with an inclined single hole and found that increasing the hole's degree of hydro erosion and conicity reduced the incidence of cavitation (see figure 4). Other results obtained in studies using real-sized single-hole nozzles can be found elsewhere [9,19,21,22].

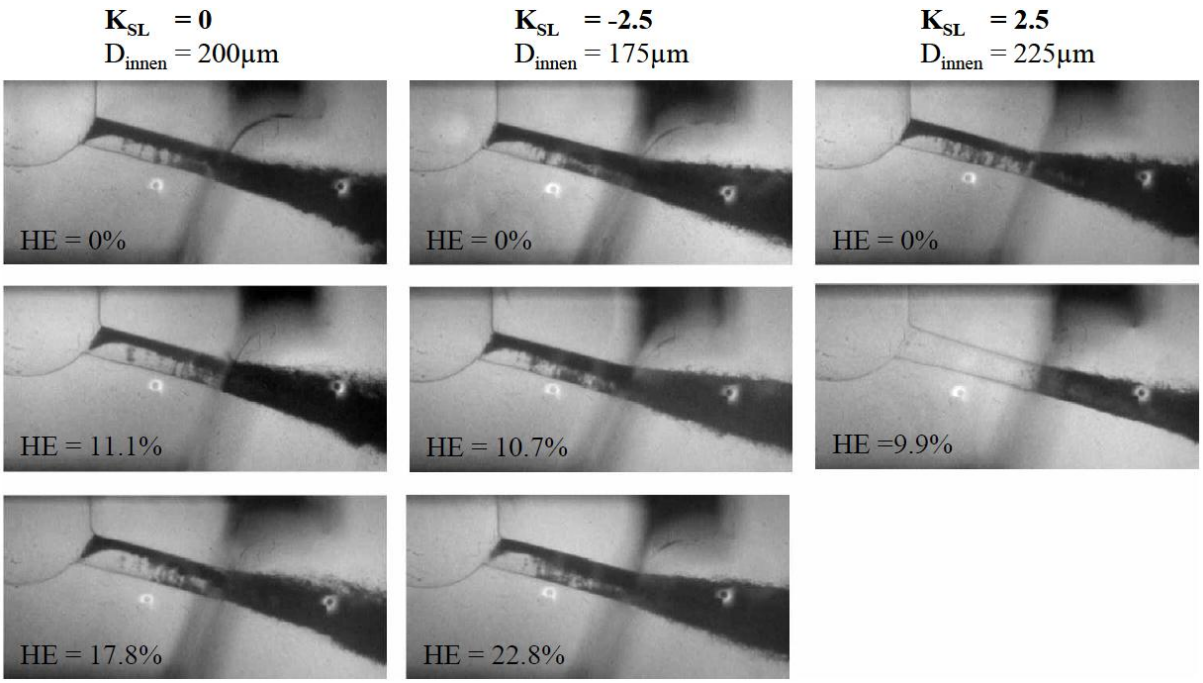

Figure 4. Nozzle hole fluid flow at full needle lift for nozzles with K-factors of 0, -2.5 and 2.5 and different grades of hydro erosion (HE). p_{RAIL}=800 bar, $p_{CHAMBER}$= 1 bar, $t_{PICTURE}$=1500µs. The conicity of the nozzles was defined as $K_{SL}= (D_{inner} - D_{exit})/10$ where D is given in µm [6].

6.4.3 Nozzle flow with real-size multi hole nozzles

Few researchers have reported studies using real-size transparent multi hole nozzles. In this context, the term “real size” refers to nozzles with hole diameters on the order of 0.25 mm or less. However, Walthers [18] conducted 3-dimensional measurements using an original-scale multi-hole transparent nozzle. An injection pressure of 300 bar was applied, with a back pressure of 1 bar. They observed three types of cavitation that were very similar to those described for up-scaled nozzles. They also mixed fluorescent particles into the fuel and measured their velocities by means of Particle Imaging Velocimetry (PIV). Their exit velocities were determined to be around 210-220 m/s in a single-hole nozzle. The 3-hole nozzle studied by Walthers generated an asymmetric velocity profile; the PIV analysis indicated that it produced a flow velocity of around 165 m/s in the upper part of the profile and 185 m/s in the lower part of the profile when using nozzle holes of the same geometrical size as that used in the single-hole nozzle. The maximum flow velocity for the 3-hole nozzle at the lower part of the entrance was around 200 m/s, but that in the upper section was appreciably lower. However, momentum exchange due to turbulence smoothened the velocity profile further downstream, reducing the maximum flow velocity to 165-185 m/s. The asymmetric flow velocity profile observed with the 3-hole nozzle was suggested to be the reason for the differences in geometrical spray height (the physical extension of the hole) and hydraulic (actual) spray height that was found in inclined nozzles and differences in spray angle of up to 3 degrees was observed by Walther *et al.* [18].

6.4.4 Nozzle damage due to cavitation

In 1979, a report by Prescher and Schaffits *et al* [23] described damage to a needle seat surface that was believed to have been caused by cavitation. The area between the seat and the needle is smaller than the total hole area during the early stages of opening and closing. The high velocity of the fuel creates a low static pressure, meaning that cavitation can occur during the opening and, perhaps more plausibly, during the closing of the needle when the flow velocity is high. The implosion of the cavitation bubbles can cause pitting on nearby surfaces. Prescher and Schaffits *et al* [23] also described damage to the hole periphery that could have been caused by film cavitation. When film cavitation occurs in the nozzle hole, it

is normally strongest at the top end. One would therefore expect the most severe wear to occur on the upper side of the nozzle hole.

6.4.5. String cavitation

The complex flow structure in the nozzle tip forms vortices between the adjacent holes and between the hole and the needle. If the pressure in the vortices is low enough, cavitation will occur and form a string of vapour between the nozzle tip and a nozzle hole [15], or between adjacent holes [16]. This form of cavitation is called string cavitation.

6.5 The discharge coefficient

At full needle lift, the major pressure drop occurs over the nozzle hole, where the fuel is accelerated by the pressure difference between the nozzle sac and the combustion chamber. The Bernoulli equation can be used to determine the maximum injection velocity, which is also known as the Bernoulli velocity:

$$v_{max} = \sqrt{\frac{\Delta p * 2}{\rho_{fuel}}}$$

Here, v_{max} is the maximum injection velocity, Δp is the pressure drop over the nozzle hole and ρ_{fuel} is the fuel density. The presence of the recirculation zone, viscous forces caused by friction, and the presence of the wall in the hole and fluid phase changes will create a pressure drop in the orifice [8,11]. Therefore the Bernoulli velocity is not achieved in reality and the real mass flow will be lower than the theoretical mass flow. The ratio of the real mass flow to the theoretical mass flow is known as the discharge coefficient, C_d.

The corrected (real) injection velocity v_c can be described in terms of v_{max} by introducing a variable, c_v, such that $v_c = c_v * v_{max}$. The effective nozzle hole area is also reduced due to the boundary layer, recirculation and cavitation. Recirculation and cavitation phenomena are dependent on the design of the hole and the injection velocity. In this context, the design of the hole includes its cross-sectional dimensions, inlet radius, flow deviation angle and wall

roughness and length. The effective flow area is described using the variable c_a such that $A_{effective} = c_a * A_{geometrical}$. The fuel mass flow through the nozzle holes can then be written:

$$\dot{m} = \rho_{fuel} * c_v * v_{\max} * c_a * A_{geometrical}$$

The discharge coefficient c_d is defined as $c_d = c_{v*} c_a$. This makes it possible to express the fuel flow through the nozzle hole as:

$$\dot{m} = \rho_{fuel} * c_d * v_{\max} * A_{geometrical}$$

The mean injection velocity is defined as:

$$v_{mean} = c_d * v_{\max}$$

or

$$v_{mean} = c_d * \sqrt{\frac{\Delta p * 2}{\rho_{fuel}}}$$

and the mass flow can be written as

$$\dot{m} = \rho_{fuel} * v_{mean} * A_{geometrical}$$

The fuel flow under stationary conditions, pressure drop and geometrical area are easily measured, making it possible to calculate the discharge coefficient. As discussed above, the mean injection velocity from a nozzle depends on the nozzle design, pressure drop and density of the fuel. The mass flow is a function of the fuel density, mean velocity and geometrical area. For a given pressure drop and fuel, the mass flow is therefore determined by the hole's geometrical area and discharge coefficient. Transient measurements of the discharge coefficient can be acquired by placing a sensor perpendicular to the path of the spray and detecting the force of its impingement [92]. The discharge coefficient can then be derived using Newton's second law of motion

$$\vec{F} = \frac{d(m\vec{v})}{dt}$$

and for the stagnation region of the sensor,

$$F_x = \dot{m} * \Delta v_x$$

where $v_x = v_{mean}$ since v_x=0 at the sensor surface. Then, given the continuity equation

$$\dot{m} = \rho_{fuel} * v_{mean} * A_{geometrical}$$

and the equation $$v_{mean} = c_d * \sqrt{\frac{\Delta p * 2}{\rho_{fuel}}}$$

c_D can be expressed as $$c_d = \sqrt{\frac{F}{2 * \Delta p * A_{geometricd}}}$$

where F is the impingement force of the spray measured just downstream of the nozzle exit.

6.6 The discharge coefficient as a function of the inlet radius

Several studies have been conducted on the relationship between cavitation, the inlet radius and the discharge coefficient [9, 24, 25, 26]. In 1959, Bergwerk [9] demonstrated that a sharp inlet edge (0 % HG) had a lower discharge coefficient than a round alternative due to the greater streamline deviations of the sharp inlet hole. Sharp inlet nozzles induce cavitation with lower cavitation numbers (CN), and the presence of edge defects can also greatly favour the onset cavitation as well as causing substantial variation in the discharge coefficient. Ohrn [26] described the discharge coefficient as a function of the inlet radius for a plain orifice. Based on analyses of nozzles with the same diameter, Ohrn concluded that the discharge coefficient for sharp nozzle inlets is controlled by cavitation and is independent of the Reynolds number for fluids with Reynolds numbers of up to 30 000. It was further shown that the discharge coefficient of a nozzle can be increased substantially by slightly increasing its inlet radius.

7. Diesel spray formation

7.1 Spray formation - atomization

Diesel engine combustion is intermittent and the time available for combustion is short. The fuel and air must therefore be mixed rapidly in order to maximize energy extraction from the fuel and thereby engine efficiency. To minimize unburned fuel, mixing must also be complete. The fuel has to vaporise before combustion, and with a large amount of small droplets the time to vaporise the fuel is short. Spray formation is the process whereby the liquid bulk emerging from the nozzle exit breaks up into ligaments and small droplets that are dispersed downstream around the liquid core. This is also sometimes referred to as atomisation. The droplets vaporise quickly and the cloud of fuel vapour is mixed with air via entrainment and engulfment. The fuel/air mixture penetrates progressively further into the combustion chamber but its velocity falls over time as it loses momentum to the surrounding air. Depending on the forces acting on the fuel and its physical properties, the break-up process can proceed under one of four different regimes. The four different regimes are the Reyleigh, first and second wind-induced, and atomisation regimes, as shown in figure 5. The atomisation regime is also known as Taylor mode. The most important properties of the fuel in relation to spray break up are its density, surface tension and dynamic viscosity. The forces acting on the fuel that play important roles in spray break up are inertial forces (aerodynamic forces), surface tension and viscous forces. The ratio of the inertial and viscous forces defines the Reynolds number:

$$\mathrm{Re} = \frac{Ud}{\nu}$$

where U is the characteristic velocity, d is the characteristic length and ν is the viscosity of the fuel. The square root of the ratio between the inertial forces and the surface tension defines the Weber number:

$$We = \frac{\rho_{fuel} U^2 d}{\sigma}$$

where ρ_{fuel} is the fuel density and σ is the surface tension [31]. The various break up regimes occupy different regions on a log-log plot of the Weber and Reynolds numbers, as shown in figure 5.

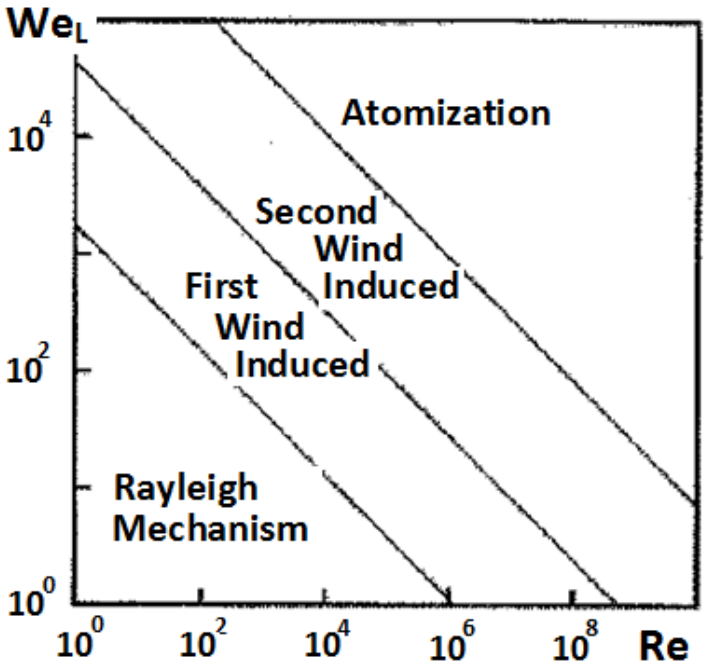

Figure 5. The four liquid jet disintegration regimes [27]

In a diesel engine, the fuel is injected at a high velocity into a high pressure and high temperature environment. The Reynolds and Weber numbers under such conditions are high, so the atomisation regime is most appropriate for describing the break up of the liquid core. Spray break-up under the atomisation regime is characterised by a rapid disruption of the liquid core, with drop formation beginning as soon as the liquid exits the nozzle and the spray starts diverging [11, 14, 21, 28, 29, 30].

The liquid core forms many small droplets whose diameter is much smaller than that of the nozzle orifice. The process is not fully understood because it is very fast and the density of the spray at this point makes it hard to investigate. It may be that the abrupt change in boundary conditions when the fuel leaves the nozzle hole creates perturbations in the form of a wave pattern with a short wavelength on the liquid surface. These waves may then grow quickly as the liquid core penetrates further [10]. The perturbations can be explained as surface instabilities caused by the difference in density between the fuel and air, which are known as Reyleigh-Taylor instabilities. Alternatively, the perturbations may be due to the transient velocities created by internal flow irregularities such as turbulence [11,32] and fluctuations in the feed pressure. Turbulence can be created by cavitation or by the pressure drop due to wall friction [11]. Wall friction creates turbulence if the flow reattaches to the nozzle wall after

passing the recirculating zone [7]. In a wavy flow region, the instability of the jet increases with the turbulence in the nozzle [12]. The surface waves of the liquid jet then grow due to aerodynamic forces [34].

When the perturbations become sufficiently large, ligaments and droplets are broken off from the core as the aerodynamic forces exceed surface tension and viscous forces. Under engine-like conditions, ligaments are observed 2-5 mm from the nozzle exit [35] and quickly break up further into droplets.

7.2 Spray characteristics

An atomising spray can be described in terms of different characteristics such as its break-up length, liquid and vapour penetration, spray cone angle and droplet size distribution. This sections briefly describes selected important spray parameters, with an emphasis on the likely effects of cavitation and turbulence on the flow.

7.2.1 Break up length

The break up length is the maximum length of the continuous liquid core emerging from the nozzle. In a previous study, break-up lengths were determined for nozzles with a range of inlet radii [34]. It was found that hydrogrinding of the nozzle increased the break up length of the spray relative to that observed with a nozzle that had not been subjected to hydrogrinding.

Han [36] measured the break up length for the sprays produced using a multi-hole nozzle at various injection pressures and found that the intact liquid core gets shorter as the injection pressure increases. This trend was attributed to increased levels of turbulence and cavitation inside the nozzle at higher injection pressures, and to more powerful aerodynamic forces that accelerate the break-up of the core. In addition, vertical single-holed nozzles were observed to produce longer liquid columns than multi-hole alternative due to the lower levels of cavitation and turbulence in the single-hole nozzle [36].

7.2.2 Liquid length

The length of the liquid plume is called liquid length and is determined by the distance between the nozzle exit and the furthest fuel droplet that has not yet vaporized. A more extended definition has been given by Johnson, J. *et al.* [60]: "Liquid length is defined as the location where the saturation temperature and partial pressure for the mixture is reached for the fuel and charge-gas mixture with ideal mixing assumed". Liquid length increases progressively after the start of injection (SOI) but if the duration of the injection is long enough, it will stabilize at a quasi-steady value. The liquid length is determined by the entrainment of hot air from the cylinder into the spray via turbulent mixing that transfers heat from the air to the fuel and vaporizing it [37]. The vapor is then further diluted and transported away from the liquid spray. The less volatile components of the diesel fuel will evaporate last and therefore determine the liquid length [37].

Several researchers have measured the relationship between the liquid length and injection pressure [37,38,39]. They have all found that the maximum liquid length is relatively independent of the injection pressure. This may be because increasing the injection pressure causes an increase in air entrainment into the spray, which would enhance its evaporation [37]. Alternatively, increasing the injection pressure may favour the formation of smaller droplets that evaporate more quickly, compensating for the increased injection velocity. The liquid length also exhibits a positive linear dependence on the orifice diameter [37], and decreases as the temperature and density of the combustion chamber gas increase [37]. Measurements of the liquid length in an optical engine yielded results that deviated from those obtained in a high pressure high temperature combustion chamber [72].

The liquid length is also known as the spray tip penetration (s). Its relationship with time (t) is initially linear since $s \sim t$. At some point during the injection, a characteristic "knee" forms in the curve, after which $s \sim t^{0.5}$ (see figure 6). The change in the curve happens when the break up length is reached and the spray is fully disintegrated into droplets. [38].

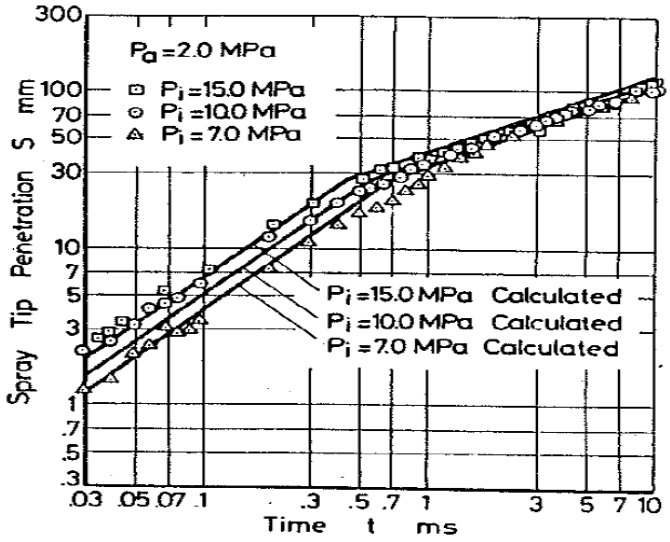

Figure 6. Spray tip penetration as a function of time [38].

As the jet penetrates, it pushes the air aside and thereby transfers momentum to it. This causes vortex formation. The loss of momentum increases when the spray reaches the droplet stage, which explains the form of the s-t curve. The droplets will exhibit varying degrees of vaporization at each point in time, and some will be pushed aside in the radial direction by upstream spray parcels with a higher velocity. Gooney [40] conducted experiments using two multi-hole nozzles with identical diameters, one having sharp inlets and the other having rounded inlets, at injection pressures of 300 to 600 bar and back-pressures of 12 to 57 bar. It was found that the spray tip penetration achieved when using sharp inlet nozzles was lower than that for the rounded inlet nozzles under all conditions.

7.2.3 Spray cone angle

The spray angle can be measured in different ways and separate definitions are required for different cases. For example, the micro spray angle close to the nozzle hole is defined by the edge of the nozzle hole and the spray in the immediate vicinity of the nozzle exit, while the macro spray angle is the full spray cone angle (see figure 7). The spray cone angle in the near-nozzle region is known as the micro angle and is determined by primary break up effects such as turbulence, cavitation, and the axial and radial velocity components. The spray cone angle for the far-nozzle region is determined by secondary break up effects such as aerodynamic effects.

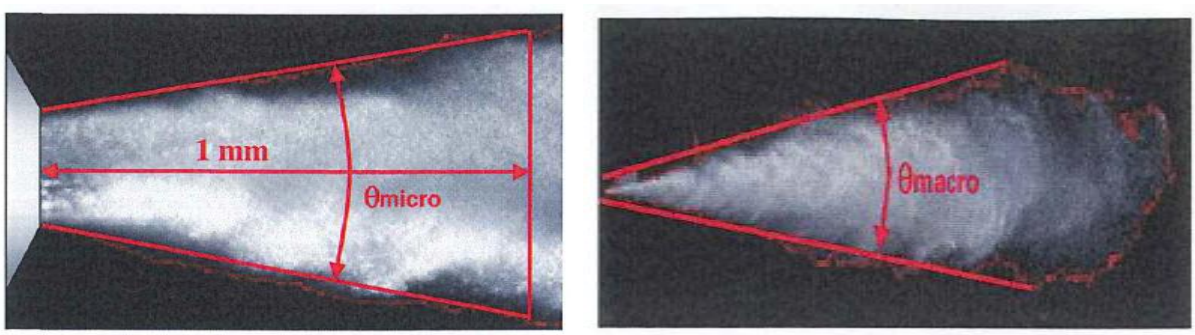

Figure 7. Spray cone angle definitions [30]

The spray angle changes during injection, partly because the throttling of the needle over the seat and the rate of fuel pressure build-up generate high velocities and turbulence in the sac and the fuel passing through the orifice [6]. Similar results have been reported by various authors [15, 36]. These phenomena are illustrated in figure 8, which compares the micro angles measured within 2 mm of the nozzle exit for a common rail system (CR) with slow needle opening and a square injection pressure profile, and a cam-driven injection system (PLD = Pumpe Leitung Düse) with rapid needle opening but gradual ramping of the injection pressure. The common rail injector produces more cavitation and turbulence at the needle seat compared to the PLD injector. Consequently, the spray angle for the common rail system is twice as large as that for the PLD injector during the opening and closing phases. However, when the needle is fully open and the bulk of the throttling occurs in the nozzle orifice, the two systems generate similar spray angles.

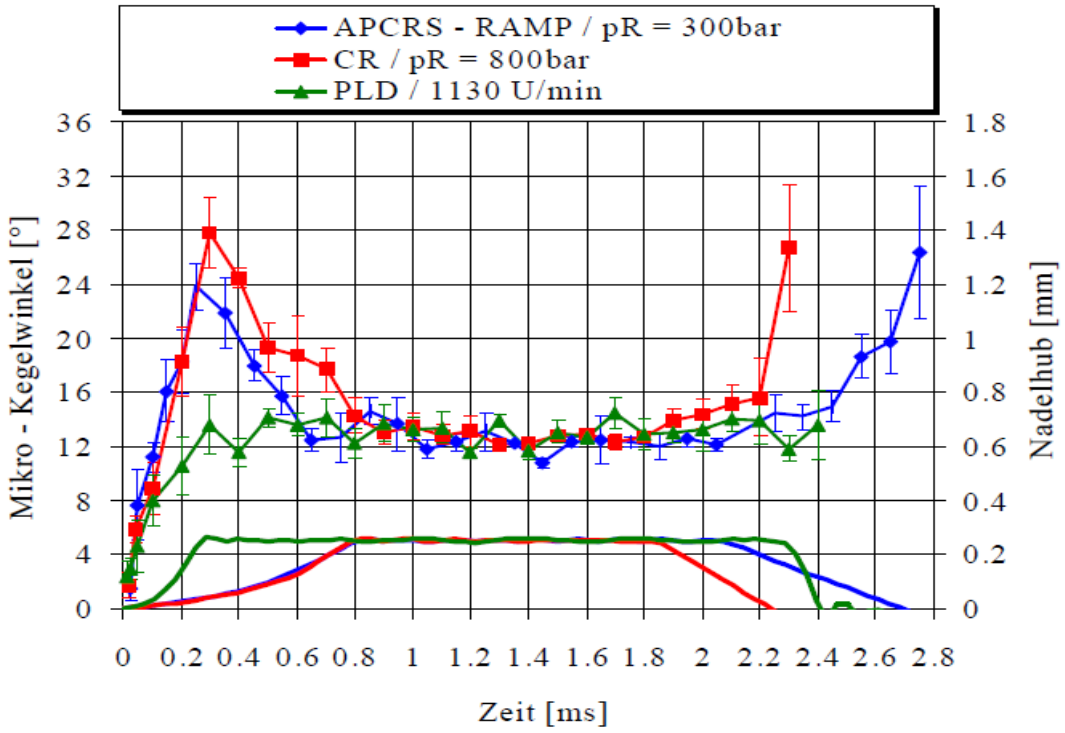

Figure 8. Comparison of micro spray angles at $T_{CHAMBER}$=293K, $p_{CHAMBER}$=21.5 bar, and $p_{INJECTION, max}$=800bar [6].

Another investigation [6] examined inclined single-hole nozzles with different conicity (K values) and grades of hydroerosion. For straight holes with K=0, nozzles that had not been subjected to hydroerosion (0% verrundet = 0% hydro erosion) produced a spray angle that was around 2 degrees greater than that for an otherwise identical nozzle that had been subjected to 17.8 % hydro erosion (17.8% verrundet in figure 9).

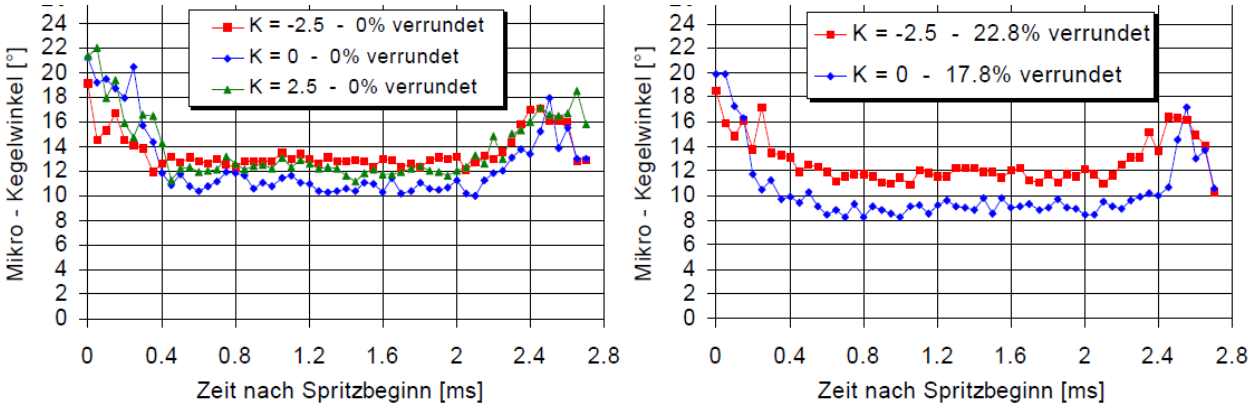

Figure 9. Comparison of micro spray angles for single-hole nozzles with different conicities and grades of hydro erosion (p_{RAIL}=800 bar, $p_{CHAMBER=}$ 1bar) [6].

A similar trend in spray angles was reported by Badock *et al.* [74] based on their studies of single-hole nozzles with different grades of hydrogrinding. They found that the spray angles for sharp nozzles were several degrees wider than those for nozzles with hydrogrinding at all points other than during the needle closing phase.

Reitz and Bracco [34] examined single-hole nozzles with different inlet radii and measured their break-up lengths. They also measured the spray cone angle in the near nozzle region in each case. A sharp inlet nozzle with no hydro grinding had a shorter break up length and a larger spray cone angle compared than a rounded nozzle inlet that had been subjected to hydrogrinding [34]. Sharp nozzles were also reported to produce larger spray cone angles when using single-holed nozzles by Ohrn [24] and Koo [41]. Reitz and Bracco focused on the spray angle in the immediate vicinity of the nozzle and only considered relatively low injection pressures (34 –172 bar). In addition, they studied a fluid with a relatively high surface tension, which would be expected to yield different results than would be seen in a diesel engine. Ohrn's studies were conducted using a low back pressure (1 bar), which produced relatively small cone angles. Ohrn concluded that the nozzle inlet has an important effect on the spray cone angle. However, the relatively weak aerodynamic forces encountered under such conditions would make the effects of flow disturbances in the injector tip much more pronounced than they would be under diesel engine-like conditions. Koo [41] also studied a system with low injection pressures (20 to 80 bar) and relatively low backpressures (1 to 20 bar). Their results also showed that sharp inlet nozzles produce larger spray angles than rounded nozzles under all conditions. However, they also demonstrated that the difference in the spray angles for the two nozzles increased with the back pressure, demonstrating that studies using low back pressures can nevertheless provide useful insights. Gooney and Corradini [40] examined several different injection pressures ranging from 300 to 600 bar, with back pressures of 12 to 57 bar. They also used multi-hole nozzles, which produce different and more engine-like flow fields and cavitation effects than those encountered with single-hole nozzles. Their results generally indicated that sharp inlet nozzles produce spray angles that are 2-4 degrees larger than those for rounded inlets. However, the difference was most pronounced at relatively low back pressures (see figure 10). These results seem to contradict Koo's findings to some extent, but all of the cited authors observed that the sharp inlet nozzles produced larger spray cone angles than their rounded counterparts. In Gooney's case, the difference between the spray cone angles for the rounded and sharp nozzles was most pronounced during the first millisecond after injection.

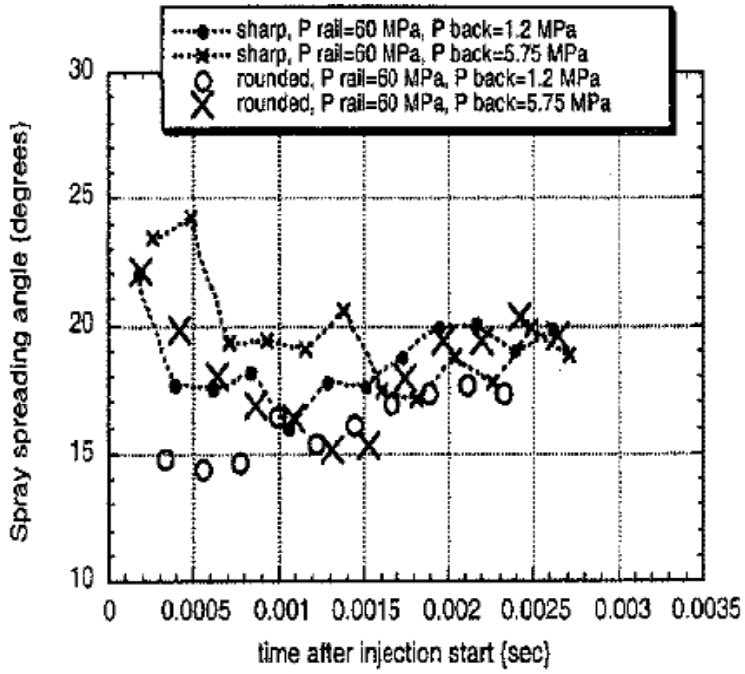

Figure 10. Spray angles for sharp and round inlets in a multi-hole injector as reported by Gooney [40].

However, by 2 milliseconds after the start of injection, the spray angles for the two nozzles had become much more similar (see figure 10). Tamaki [42] studied different operating conditions and did not reported any spray cone angle measurements but did publish a series of photos suggesting once again that sharp inlet nozzles produce larger spray angles than rounded equivalents. Finally, the engine measurements reported by Borthwick and Farrell [72] indicate that the spray angle can vary significantly between engine cycles, so it is necessary to take multiple measurements and average them in order to obtain reliable results.

Badock [22] also measured spray cone angles generated using single-hole nozzles with injection pressures of 250 to 600 bar and a 1 bar backpressure. One sharp and two rounded nozzles were studied, and the two nozzles with the most pronounced differences in their spray angles were those with the rounded inlets: their spray angles differed by 1-3 degrees over the bulk of the studied period. Badock concluded that the nozzle hole inlet radii had no significant effect on primary spray break-up. Kampmann [43] studied multi-hole nozzles with a 600 bar injection pressure and an engine-like backpressure. They measured the spray cone angles generated using sharp and rounded inlet nozzles and reported that their spray cone angles differed by around 0.5 degrees. The statistical variation in the test results was on the same

order, so there was no significant difference between the results for the sharp and rounded nozzles. Su and Farell [44] compared multi-hole nozzles with sharp and rounded inlets but identical diameters at a chamber pressure of 16 bar and injection pressures of 720 to 1600 bar, and measured the resulting spray cone angles (along with several other parameters). They found that the sharp inlets produced a spray angle that was 1-4 degrees wider than that for the rounded inlets at the same injection pressure during the first 1 to 3 milliseconds after SOI. When the flows through the nozzles were equalized (which required the use of a lower injection pressure for the rounded inlets), the spray angles were similar or up to 3 degrees larger for the sharp inlet nozzle. These findings were confirmed in another study also reported by Su and Farell [45].

The measured spray cone angle may also depend on the perspective from which the spray is observed. Heimgärtner [46] reported that the spray angle determined from a side view was greater than that determined from the front/top view. This is because internal flow effects can create asymmetric flow profiles in the nozzles due to the recirculation zone. Because these effects depend on the angle between the nozzle hole axis and the needle axis, they become stronger when the angle between these axes decreases or the spray hole cone angle increases. Heimgärtner also observed that the spray angle increased with the angle of inclination between the spray hole axis and the needle axis (see figure 11).

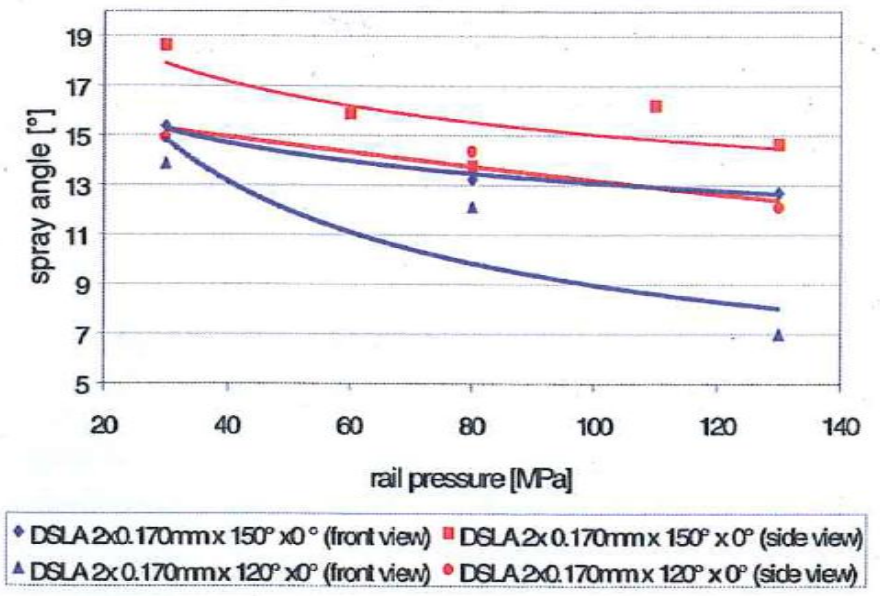

Figure 11. Comparison of spray angles determined from the front (top) and side views, as reported by Heimgärtner [46]

Other authors have reported spray angle results related to cavitation. Payri observed that when using a multi-hole nozzle, a larger spray cone angle was measured when cavitation was observed [79]. Desantes used an axisymetrical single hole [80] and reported a spray angle increase of about 2 degress when the flow was cavitating.

7.2.4 Drop size

The atomisation process generates many small droplets. They are not perfectly spherical so their diameter must be defined based on the total volume of all of the droplets. One way of averaging the drop size is to calculate the Sauter Mean Diameter (SMD), which is defined as:

$$D_{32} = \sum_{i=1}^{i=N} D_i^3 / \sum_{i=1}^{i=N} D_i^2$$

Essentially, the sum of the volumes of the individual droplets is divided by the sum of their projected areas.

The literature data on the measured drop sizes generated using nozzles with and without hydro grinding are varied. Gooney [40] used nozzles with identical diameters, but focused on the injection of diesel fuel under engine-like conditions. With a 600 bar injection pressure, they observed a SMD for sharp nozzles of around 30-40 μm compared to 25-30 μm for the rounded inlet nozzle. Su and Farrell also used sharp and rounded nozzles with identical diameters with engine-like injection pressures (720 to 1600 bar) and a backpressure of 16 bar. However, they adjusted the injection pressures in their experiments in order to achieve similar flow levels through the different nozzles. Under such conditions, the average SMD for the rounded nozzles was only a micrometer or two larger than for the sharp nozzles. However, if the injection pressure was kept constant, the SMD was a micrometer or two larger for the sharp inlet nozzle. The droplet size ranged from 25 to 35 μm [44]. Koo [62] used diesel fuel with injection and back pressures of 106 bar and 6 bar, respectively, and reported SMD values at various axial and radial positions within the combustion chamber. The sharp and round inlet nozzles yielded similar droplet diameters and the measurement curves overlapped fairly well. The measured droplet sizes ranged from 20 to 120 μm. Overall, it seems that at a given

injection pressure, sharp inlet nozzles tend to produce larger droplets. This may be due to aerodynamic effects arising from their comparatively low injection velocities.

7.3 The effect of hydro grinding/hydro erosion on injection velocity

Increasing a nozzle's inlet radius will raise its discharge coefficient, making the fuel velocity field more symmetrical and reducing the fluid's cavitation intensity [77] and turbulence kinetic energy [43]. Spray propagation velocities have been measured in optical engines [43,88] at both constant injection pressures and constant fuel flows. Kampmann *et al.* [43] reported that a nozzle subjected to 20% hydrogrinding generated velocities that were up to 50 % greater than those for a nozzle with 0% hydrogrinding (see figure 12). Schmid *et al.* [88] reported significantly faster spray velocities for nozzles with higher discharge coefficients due to hydrogrinding and increased conicity, as shown by the diagram and spray contours presented in figure 12. Increasing the degree of hydrogrinding applied to the nozzle inlet will reduce the spray cone angle [74] and the deviation of the dynamic spray angle from the geometrical spray angle [18]. In studies using an optical engine and impingement measuring apparatus, Kampmann *et al.* [43] observed that nozzles with hydrogrinding generated significantly increased mean injection pressures and momentum values. Schmid [88] also conducted studies using an optical engine and observed significantly higher injection velocities and increased spreading of the flame after impingement on the piston bowl walls due to hydrogrinding.

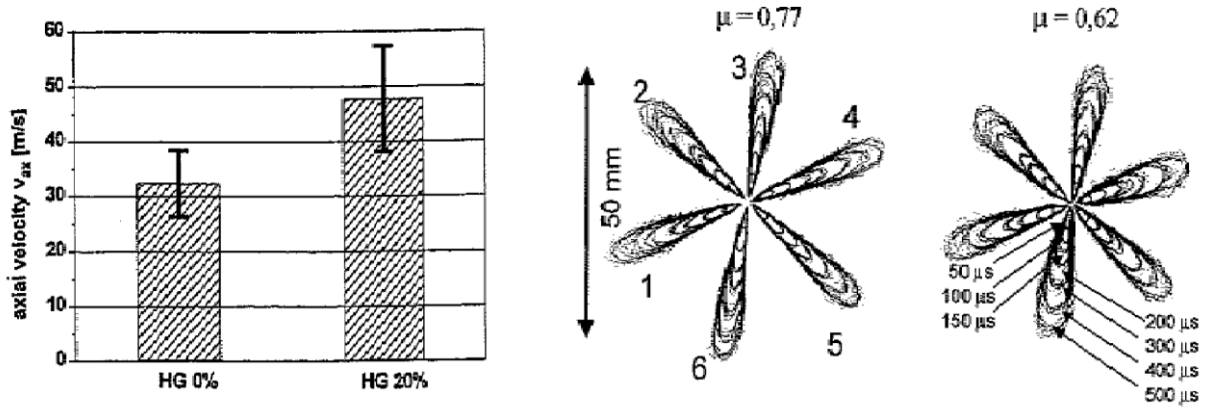

Figure 12. Left: Spray velocities generated by two nozzles with different degrees of hydrogrinding (HG) according to Kampmann [43]. Right: The development of spray contours generated using nozzles with different discharge coefficients (μ) according to Schmid [88].

8. Combustion and emission formation in diesel sprays

8.1 Introduction

Combustion in diesel engines is a complex process that occurs over a very short period of time. It is difficult to acquire measurements inside the engine due to its high operating temperature and pressure. Therefore, in previous years, combustion and emission formation models were based primarily on results obtained under non-engine like conditions and exhaust measurements. In 1996 a break-through in diesel spray combustion theory was presented by Chomiak and Karlsson [47]. Their spray combustion model included a description of air entrainment in the lift off region and predicted the occurrence a pre-mixed flame called triple flame just downstream of the lift off length, in which a significant portion of the heat release takes place. In 1997 a conceptual combustion and emission formation model similar to that of Chomiak and Karlsson was presented by Dec [48]. Unaware of the work of Chomiak and Karlsson, the Dec model was based on data gathered using laser measurements. It describes the pre-mixed flame as well as the formation of soot and NO_x. The advantages of laser based measurements are the temporal and spatial resolution and the possibility to measure combustion related species inside the engine without major interference with the combustion process. Subsequent investigations have provided further insights into the diesel spray combustion process.

8.2 Dec's conceptual model

Soon after the start of injection (ASI), vapor appears about half way along the downstream section of the liquid stream (Figure 13). At 3º ASI, light from chemical reactions appears in the vapor region, although the rate of heat release remains negative due to strong evaporation. Between 4.5º ASI and 5º ASI the fuel breaks down in the jet cross section almost uniformly and this coincides with appearance of PAH formed in the same region. The fuel equivalence ratio in the fuel break down region is around 2-4. Because the timing of the major fuel break down coincides with the start of the rapid rise in the heat release rate at the start of the premixed combustion, it indicates that the majority of the premixed combustion is fuel rich. Premixed combustion occurs volumetrically throughout the cross section of the leading portion of the jet. Soot occurs as very small particles from the fuel rich premixed combustion

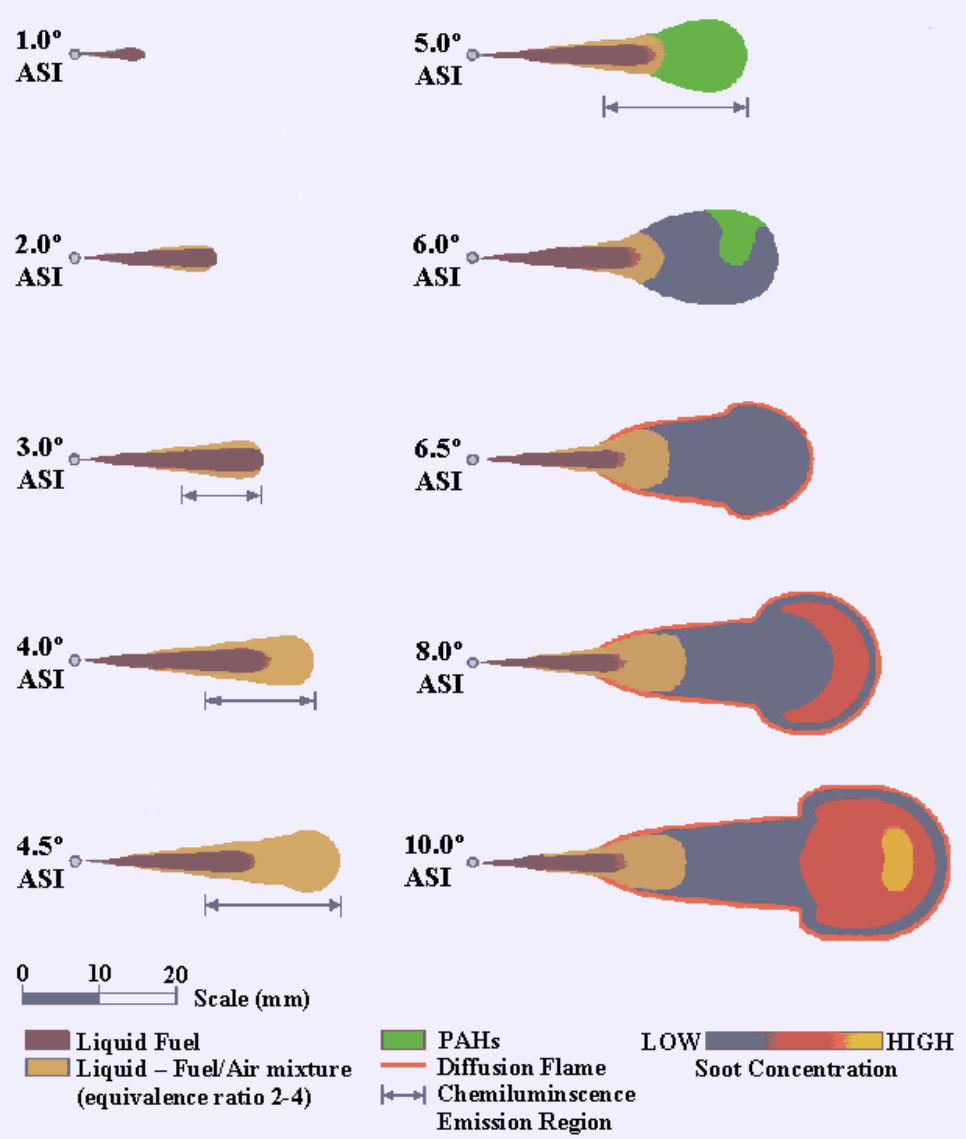

Figure 13. A temporal sequence showing the initial steps of DI diesel spray combustion [48].

at 6º ASI. This occurred 140 μs after the PAH signal was first detected, showing that the soot formation process is very fast. At 6.5º ASI, soot is found throughout the cross section of the leading portion of the jet. Between 5.5 to 6.5º ASI, mixing-controlled combustion starts to occur around the jet, as demonstrated by the levels of OH radicals. At 7 to 9º ASI, the soot concentration increases in the cross section of the sooting region, especially at the leading edge where the largest particles are found. The larger particles at the periphery are believed to be generated by mixing controlled combustion. When mixing controlled combustion starts (~9º ASI), the appearance of the jet does not differ greatly from that during the late stages of

premixed combustion. The soot concentration starts at a fixed point and increases downstream of the jet, peaking in the head vortex.

Figure 14 shows a conceptual model for mixing-controlled combustion. Soot formation occurs in the entire jet cross section downstream of a point at an almost fixed distance from the nozzle. Hot air is entrained in the lift off region. Lift off length the distance from the nozzle to the high temperature zone determined by OH chemiluminiscence that is regarded as a good marker for high temperature [58]. The hot air has a temperature of around 950 K and mixes with the fuel to form a fuel/air mixture with a temperature of about 825 K. This is not hot enough for soot formation, which requires temperatures of around 1300 K. A fuel rich premixed flame due to the flame lift off is suggested to form the soot particles in the plume. The premixed flame releases a significant fraction of the total heat of combustion, which depends on the amount of air entrained into the spray. The premixed flame is suggested to have a fuel equivalence ratio of about 4, which would support soot formation at its temperature of around 1600 K. This means that all of the fuel passes through a zone where fuel rich premixed combustion is occurring. Fuel that does not burn in this zone is later burned in a diffusion flame.

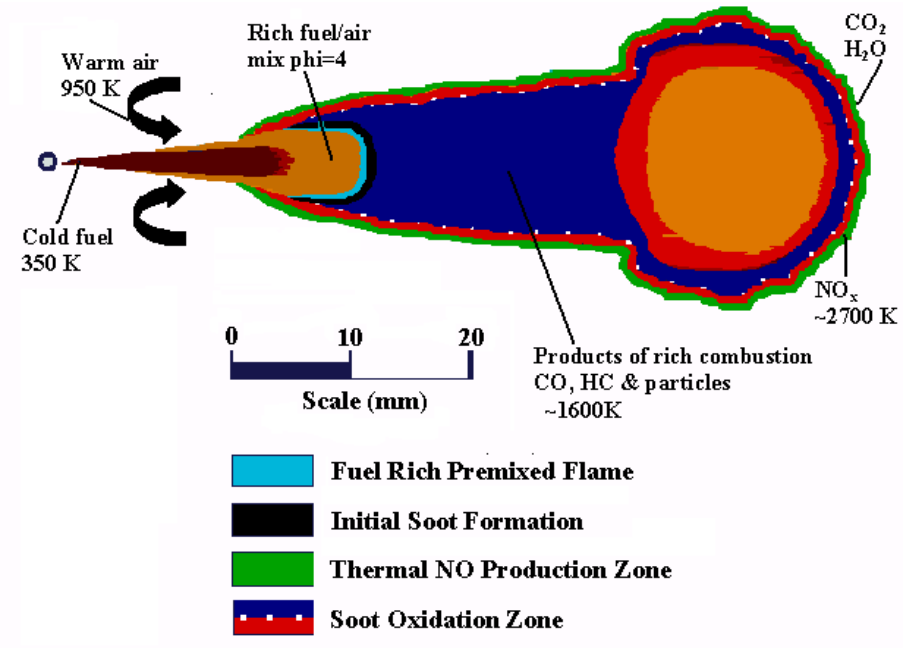

Figure 14. An illustration of the fuel burning processes, from reference [49].

Soot oxidation takes place in the diffusion flame, which is the only location where OH radicals are found. OH radicals are generated by combustion under near-stoichiometric conditions. Oxygen from the surrounding air will also oxidize soot if the temperature is high enough. The temperature of the diffusion flame is around 2700 K, which is sufficient to form NO_x. CO_2 and H_2O are formed in the diffusion flame.

8.3 Air entrainment

Cooling effects due to fuel vaporization and quenching due to the shear arising from the high injection velocity gradients lift the flame from the nozzle. At this point, the local flame speed and thermal diffusivity are balanced against the turbulent mixing as well as the effects of the ambient temperature and pressure. The amount of air entrained into the spray in the lift off region has a significant impact on the spray's combustion. Bearing the combustion model from figure 14 in mind, increasing the amount of air entrainment will lean out the fuel-rich premixed flame in the core of the jet. Figure 14 shows a developed flame burning under quasi-steady conditions. The rate of air entrainment, $\dot{m}_a$ is suggested to be proportional to the density of ambient air (ρ_a), hole diameter (d), injection velocity (v_{mean}) and spray angle (θ) according to the following expression [50]:

$$\dot{m}_a \sim \rho_a * d * v_{mean} * \tan(\Theta/2)$$

The air entrainment in relation to the injected fuel rate can be described using the percentage of stoichiometry (ξ_{St}), were 100% would represent stoichiometric condition. Figure 15 shows a plot of the percentage of stoichiometry as a function of the nozzle hole pressure drop and hole diameter for a free single spray [51]. The percentage of stoichiometry clearly increases with the pressure drop and is strongly dependent on the hole diameter. Siebers et al. [68] reported that on a percentage basis, ξ_{St} is 4 to 5 times more sensitive to a change in orifice diameter than a change in orifice pressure drop. The properties of the gas into which the fuel is injected, such as its temperature, pressure and oxygen concentration also affect the lift off length (and therefore air entrainment) [59].

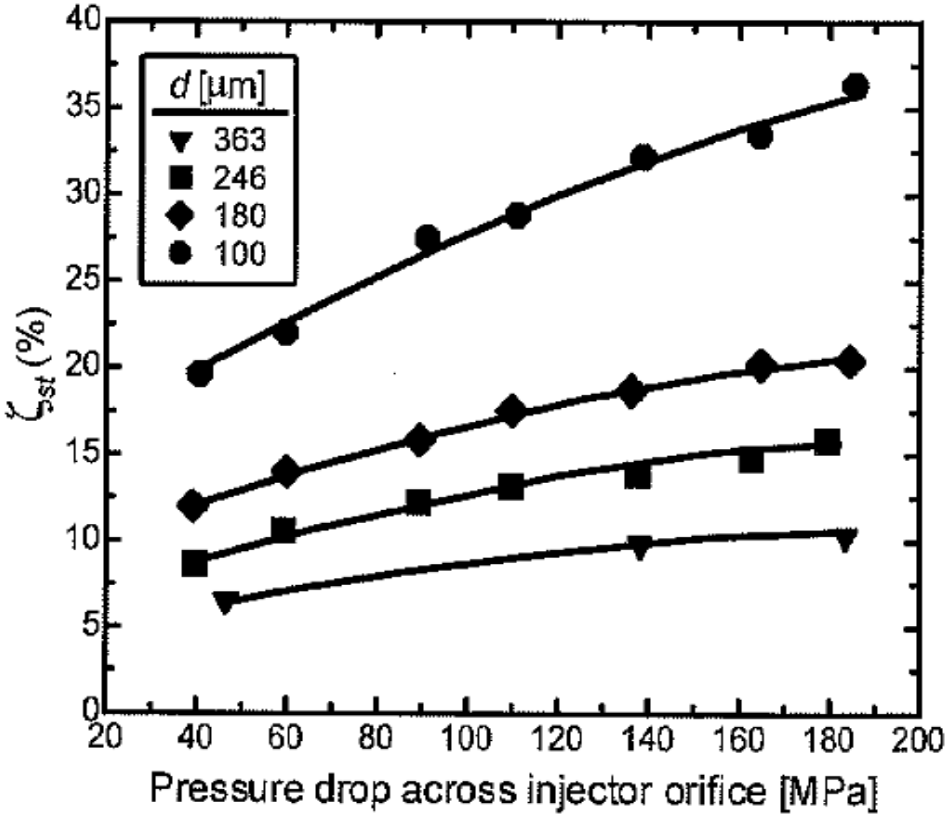

Figure 15. The estimated percent of stoichiometric air entrained upstream of the lift-off length (ζ_{st}) as a function of nozzle orifice pressure drop and hole diameter [51].

Pickett [52] investigated the effects of soot incandescence at various levels of air entrainment using a axisymmetric single hole nozzle in a high pressure high temperature chamber. Figure 16 shows a plot of the soot incandescence normalized against the fuel flow rate for orifices of various diameters, as a function of the percentage of stoichiometric air (ξ_{St}) with a nozzle pressure drop of 1380 bar. The soot incandescence decreases as ξ_{St} increases; once the percentage of stoichiometric air reaches around 44 %, no soot incandescence is observed. Other studies have also shown that soot formation stops once the fuel/air ratio reaches a value of around 2 or more, which is equivalent to 50% stoichiometry [4, 51, 53].

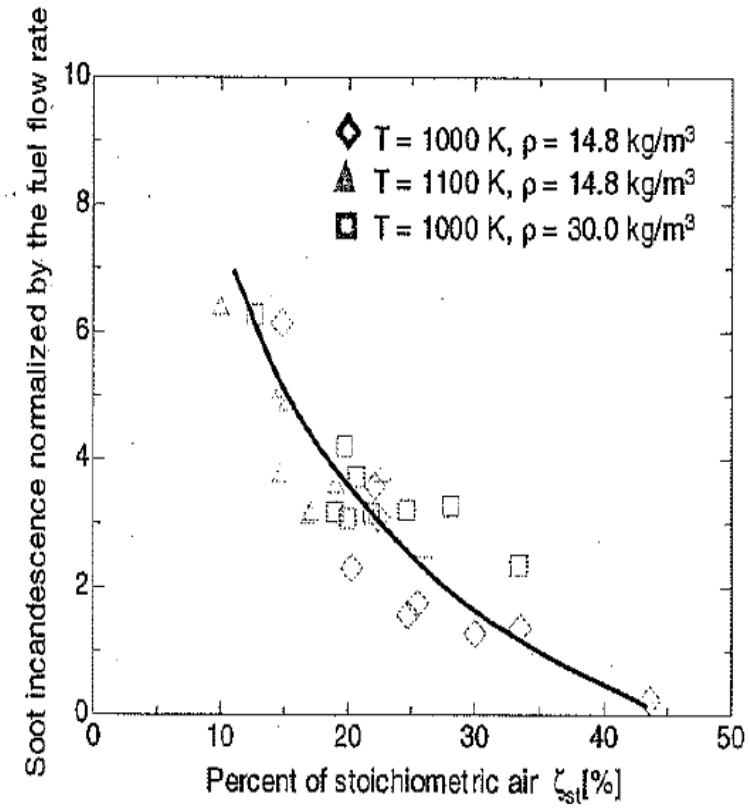

Figure 16 Total soot incandescence (normalized against the fuel flow rate) as a function of the percentage of stoichiometric air ζ_{st} (%) entrained upstream of the lift off length.

If the oxygen content of the gas falls, which will happen if exhaust gas recirculation is used, the lift off length will increase. However, the amount of oxygen entrained into the spray is not significantly reduced because the reduced oxygen content of the in-cylinder gas is offset by the increased lift off length [67]. The lift off length can vary substantially: in an engine experiment reported by Musculus [66], it varied by up to 30% between experimental runs. This variation may be due to the effects of residual combustion products, which would have a lower oxygen concentration than the ambient air.

Figure 17 shows a diagram illustrating the soot and NO_x formation regions as functions of temperature and the local equivalence ratio (i.e. the fuel/air ratio, ϕ). As the degree of air entrainment increases, the pre-mixed flame from the conceptual model gets leaned out and there is less scope for soot formation in the downstream zone of the spray plume. Consequently, there is less soot and smaller quantities of other cracked fuel derivatives to be oxidized in the diffusion flame. In the diffusion flame the soot, fuel and cracked derivatives

burn under approximately stoichiometric conditions, and high temperatures are reached. These high temperatures favor NO_x formation.

The red line in figure 17 describes the pathway taken by an imaginary fuel/air parcel as it leaves the injector nozzle hole, vaporizes, mixes with air, burns, and gets diluted. Starting in the top left corner, the fuel has just left the nozzle hole at a temperature of around 300 °C and been mixed with air to give an equivalence ratio of 6. When the parcel reaches the point at which all of the fuel is vaporized (at an equivalence ratio of 4), its temperature is around 500 °C. Shortly after, the mixture ignites a premixed flame is formed and the temperature increases rapidly so that soot is formed. Soot concentration increases but when the parcel approaches the diffusion flame and is leaned out by entrained and engulfed air. Because reactions occur between fuel and its transformed components and oxygen the temperature is rising. Peak temperature is reached at ϕ=1.05 and NO_x emissions are formed where there are excess air and high temperatures. With further dilution by air and combustion products temperatures drop and reaction rate decrease and NO_x emission production will cease before soot oxidation. With sufficient mixing, it is therefore possible to oxidize soot late in the combustion cycle without increase NO_x emissions.

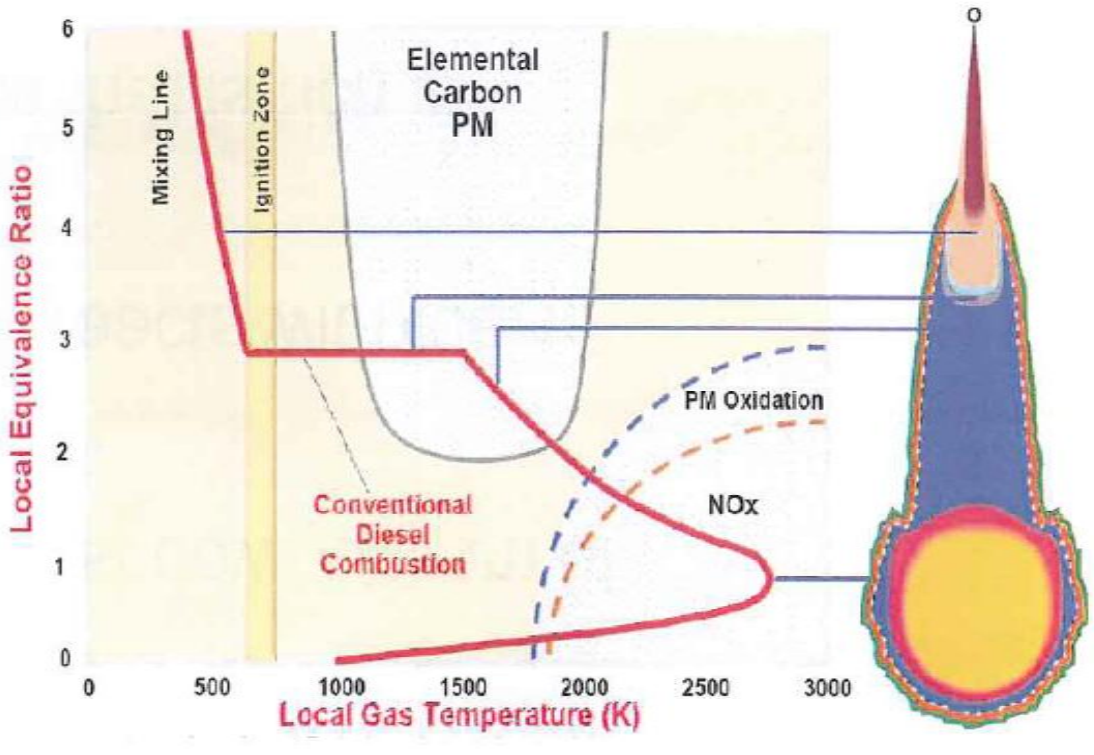

Figure 17. Soot and NO formation as functions of the fuel-air ratio and local gas temperature [89].

8.4 Wall impingement

Because the combustion chamber is a confined space, the flame will inevitably interact with its walls. The wall that the flame normally hits first is that of the piston bowl, as shown in figure 2. The impact does not immediately extinguish the flame, however. Dec [69] measured a delay of 70 µs before the flame was quenched. The flame thus stands off the wall and consumes the available oxygen before being quenched. The quenching is due to a high rate of heat loss, radical depletion, and an insufficient supply of oxygen. The soot particles in the jet at this point are small and move with the gas flow. The vast majority of the soot will flow off to the sides and be consumed by oxidants. However, some is deposited on the piston bowl wall, primarily at the location where it is struck by the leading edge of the jet [69]. The boundary layer is thin and soot can be pushed through it, possibly by thermophoresis [70]. Because the side of the particle that is facing towards the flame will be the hottest, it will form more interactions with gas molecules on this side. This creates a stronger contact force on the warmer side, pushing the particle towards the cold side – in this case, the wall. Similar physical processes were found to be responsible for soot-mediated oil thickening as the flame and combustion gases impinge on the cylinder liner [71].

8.5 Soot formation

Soot formation in a diesel engine is a complicated process that occurs over several steps, many of which are not fully understood. In figures 18 and 19 the soot formation process is schematically outlined. It begins with pyrolysis, a process in which fuel molecules are cracked into progressively smaller fractions that can participate in a wide range of reactions. These reactions form larger molecules such as aromatic and polyaromatic compounds that are stable at relatively high temperatures, as well as acetylene and its higher analogues ($C_{2n}H_2$). These two types of hydrocarbons seem to be the main gas-phase precursors of soot [4]. Nucleation causes the transfer of mass from the gas phase to the particulate phase as gas-phase precursors condense and combine to form small particles. Nucleation is followed by surface growth, in which acetylene is incorporated into new aromatic rings that are added to the surface of the nuclei. This surface growth generates the bulk of the soot mass. Agglomeration is a process whereby two particles merge. There are three types of agglomeration. The first is called coagulation and occurs during the early stages of particle growth when two spherical particles may combine to form a single spheroid. Its spherical shape may be restored due to rapid

surface growth. The second type of agglomeration occurs when the spherules have solidified before collision and their surface growth rates have diminished. The resulting particles form a cluster in which the individual spherules can be seen. The third type is called aggregation. This is when the surface growth has ceased and the individual spherules form a chainlike structure. These particle chains are known to carry a positive charge, which has been suggested to be responsible for their chainlike structure [4], [54]. Examples of agglomerated particles are shown in Figures 21 and 22.

As shown in Figure 18, all of these steps also involve oxidation and several species are known to oxidize soot, e.g. O, OH, O_2 and H_2O. If such oxidants are present and the temperature is sufficiently high, the soot particles will be oxidized. The reaction probabilities for O and OH radicals are at least one order of magnitude higher than those for O_2 and H_2O. The mechanism for the reaction between the OH radical and carbon is as follows:

$$C + OH \rightarrow CO + H$$

This reaction itself is only weakly dependent on the temperatures, but the concentration of OH is very temperature-dependent.

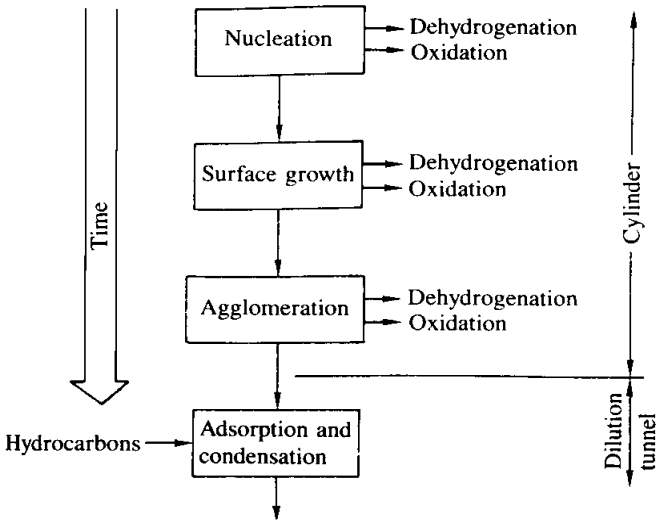

Figure 18. Processes leading to the net production of diesel particles [4].

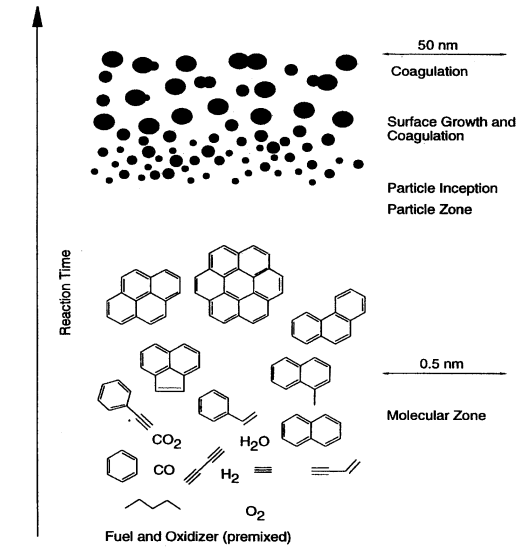

Figure 19. The reaction path leading to soot formation [55].

8.6 Soot particles

The soot formed in flames generally contains at least 1% by weight of hydrogen. On an atomic basis, this represents quite a considerable proportion of this element, giving the soot an approximate empirical formula of C_8H. When examined under an electron microscope, the deposited soot appears to consist of numerous approximately spherical particles called spherules that are strung together like pearls on a necklace. The diameters of these spherules range from 10 to 200 nm but are usually between 10 and 50 nm (see Figures 21 and 22). The smallest particles are found in luminous but non-sooting flames, while the largest occur in heavily sooting flames. X-ray diffraction analyses have shown that each particle is made up of many (10^4) of crystallites, as shown in Figure 20.

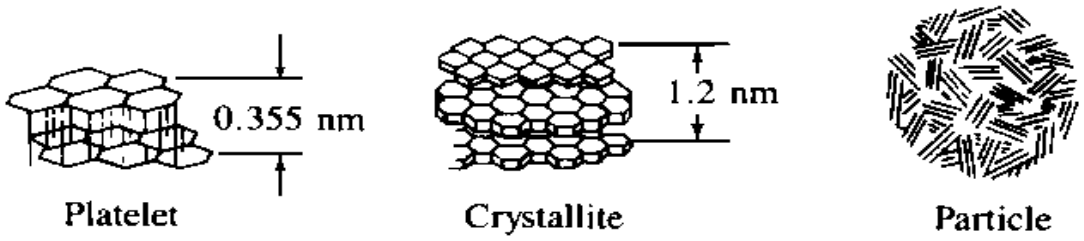

Figure 20. Carbon particle substructure [4].

Electron diffraction studies have shown that each crystallite consists of 5-10 sheets of carbon atoms (of the basic type found in ideal graphite), each containing about 100 carbon atoms and thus having a length and breadth of the order of 2-3 nm. However, while the layer planes are parallel to one another and separated by a constant distance in the same way as in graphite, they have a turbostratic structure. That is to say, they are stacked randomly in relation to one another, so the interlayer spacing of 0.355 nm is greater than that of 0.335 nm for ideal graphite. An "average" spherical particle contains between 10^5 and 10^6 carbon atoms [56].

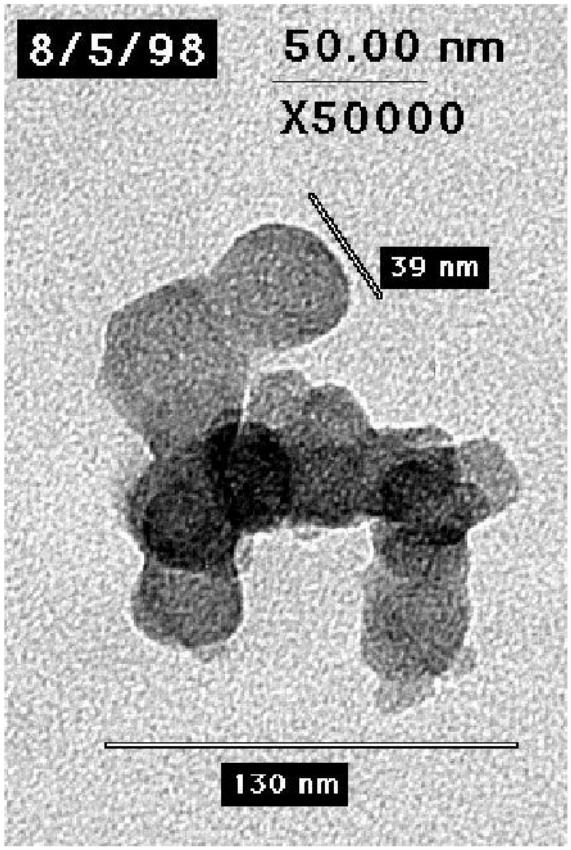

Figure 21. Representative particles [57].

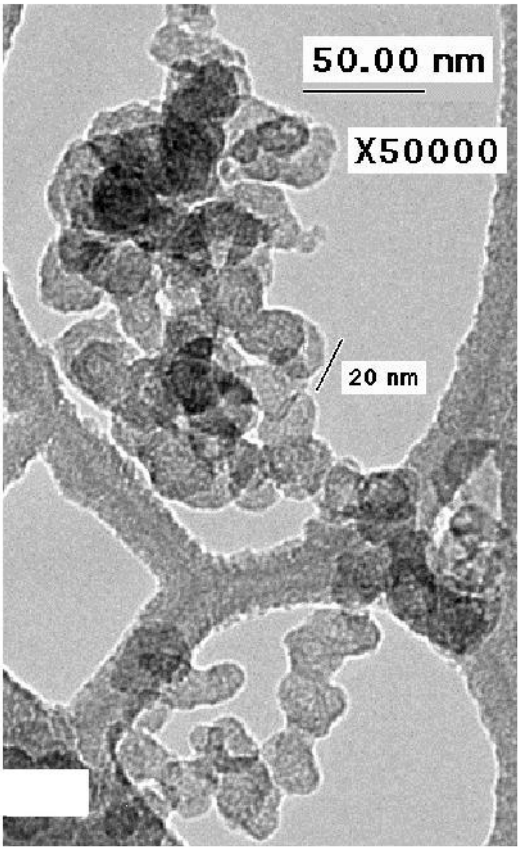

Figure 22. Representative particles [57].

8.7 Engine out soot emissions

The mass flow of soot in the engine exhaust depends on two competing processes: soot formation and soot oxidation. Soot formation increases with the mass of injected fuel; because soot is formed in rich regions and oxidized in regions that are sufficiently hot and slightly leaner than stoichiometry, the rate of oxidation peaks after the peak of soot formation. Time resolved in-cylinder sampling has shown that most of the soot produced in the engine is oxidized before exhaust valve opening [90, 91].

8.8 NO_x formation

NO_x is a catch-all term that refers to both NO and NO_2, It can be formed by at least three mechanisms: fuel, prompt, and thermal.

Fuel NO_x is formed when the fuel contains nitrogen. Since the amount of nitrogen in diesel fuel is very low, this mechanism can be neglected when studying diesel engines [56].

Prompt NO_x is formed by reactions between molecular nitrogen, N_2, and radicals such as C, CH, and CH_2 that are derived from the fuel. These reactions results in the formation of fixed nitrogen species such as NH (nitrogen monohydride), HCN (hydrogen cyanide), H_2CN (dihydrogen cyanide) and CN- (the cyano radical), which can subsequently be oxidized to form NO [56].

The thermal mechanism is thought to be the dominant source of NO_x formation in diesel engines. Thermal NO_x is formed when air is exposed to high enough temperatures for a long enough time. Its rate increases exponentially with the temperature, so thermal NO_x formation primarily occurs near the combustion zone. The rate of thermal NO_x formation can be calculated by considering the extended Zeldovish mechanism reactions, which are:

$$N_2 + O <-> NO + N$$
$$N + O_2 <-> NO + O$$
$$N + OH <-> NO + H$$

8.9 The particle - NO_x trade off

The timing at which the fuel is injected into the engine in relation to the position of the piston, determines the temperature and pressure at which the fuel will be combusted, as well as the time the combustion process will take and how the fuel jet will interact with the walls. If the fuel is injected late in the compression stroke, which can be regarded as an early injection timing, the fuel will burn at relatively high temperatures over a long period of time. If the fuel is injected early in the expansion stroke, which can be regarded as a late injection timing, the fuel will burn at relatively low temperatures for a short time. Exposure to high temperatures for a long time will cause increased NO_x production but also favour the oxidation of particulate matter, provided that there are adequate oxidants available. Combustion at low temperatures over short periods of time will reduce NO_x production but also suppress the oxidation of particulate matter, resulting in high particle emissions. By varying the injection timing for a given fuel flow and engine speed, one can construct a trade-off curve between particles and NO_x emissions. Typically, particle densities are measured with a smoke meter and examples of a smoke-NO_x emissions trade off curves are found in figure 30.

9. Engine experimental equipment

9.1 The engine

All engine tests were conducted using a single-cylinder engine manufactured by AVL. The engine was supplied with a Volvo cylinder head based on the D12C engine and was equipped with a Lucas EUI 200 A3 electronic unit injector (EUI). It was fed with pressurized air from an Atlas Copco GA55W compressor; the air was dried before use. The only fuel used in the experiments was Diesel fuel. The specifications of the fuel and the emission measurement equipment used in the engine experiments are discussed in detail in the corresponding papers.

9.2 Engine optical studies

One part of this thesis work involved a redesign of the engine's cylinder head. The aim was to maximize optical access to the cylinder while still being able to use the engine under normal operating conditions, and caution had to be taken to ensure there was enough wall thickness around the hole that was to provide the optical access. This was achieved by removing one exhaust valve from the 4-valve head and recasting the cylinder head. The hole was machined with an inclination of 10 degrees from the vertical axis to create a wide range of viewing options, as shown in figure 23. Two different sleeves were designed to be inserted into this hole from above and screwed into the cylinder head. A quartz window was glued to the bottom of each sleeve using high-temperature silicon. In one sleeve design, the window had a straight cylindrical fit, while in the other the window had a conical fit. The windows were mounted from the bottom up in the sleeve, with only the silicon holding the window in place. The window's surface flush to the cylinder head was slightly elliptical due to the inclination of the hole; the diameters of the glass were 43*42 mm (see figure 23).

The valve cover was redesigned such that the cover would prevent engine oil from entering into the sleeve. Nevertheless, it was possible to stick a camera lens or long distance microscope into the sleeve at the height of the cylinder head in order to acquire close up images. The valve train has one cam shaft, and it was the exhaust valve furthest away from the camshaft that was removed. The original engine design features a single rocker arm that acts on both exhaust valves. The arm's lever contact point is located between the exhaust

valves and acts on a yoke, which presses down on the two valves. With only the closest valve remaining and the yoke removed, a shorter lever was designed on the new rocker arm. To compensate for the reduced valve lift, a new exhaust cam had to be designed. By using a much steeper and higher cam profile, it was possible to achieve almost the same lift curve as the original design at the expense of giving the new cam a shorter expected life time than the original. Because the modified engine has only one exhaust valve, the amount of residual gas in the engine will increase. Gas exchange calculations indicated that the amount of residual gas retained in the modified engine is approximately twice that for the original design as seen in Table 1.

Table 1. Calculated residual gas fractions with 1 and 2 exhaust valves for selected cases

Engine speed (rps)	load (%)	Pin(bar)	Pexh (bar)	Mfuel (kg/h)	EGR 2 exhaust valves (%)	EGR 1 exhaust valves (%)
25	50	1,67	1,54	4,69	3,5	7,2
25	100	2,58	2,07	8,93	3	5,3
30	50	1,81	1,76	5,23	4,2	10
30	100	2,6	2,44	10,08	3,9	6,6

The strength of the materials in the optical cylinder head was sufficient for the tested engine operation conditions, although some small chips were lost from the glass window. However fouling of the window was a major problem because the piston directed the spray up towards the glass and running time was maximum ½ minutes before fouling was too heavy. Every time the window was cleaned, it was necessary to inspect the integrity of the silicon holding the glass in place because if became too weak, gravity would pull the window down into the engine. Eventually, it was determined that the strength of the bond could be estimated by judging how much of the silicon had separated, allowing the formation of a thin layer of air between the glass and the silicon. Once this area had grown beyond a certain point, the glass could be pressed out for cleaning and then glued back into the sleeve with new silicon. Acetone was used to degrease the sleeve and the glass to strengthen the bond formed by the silicon. The modified cylinder head was used in the studies presented in Paper 3 (SAE 2002-01-2671).

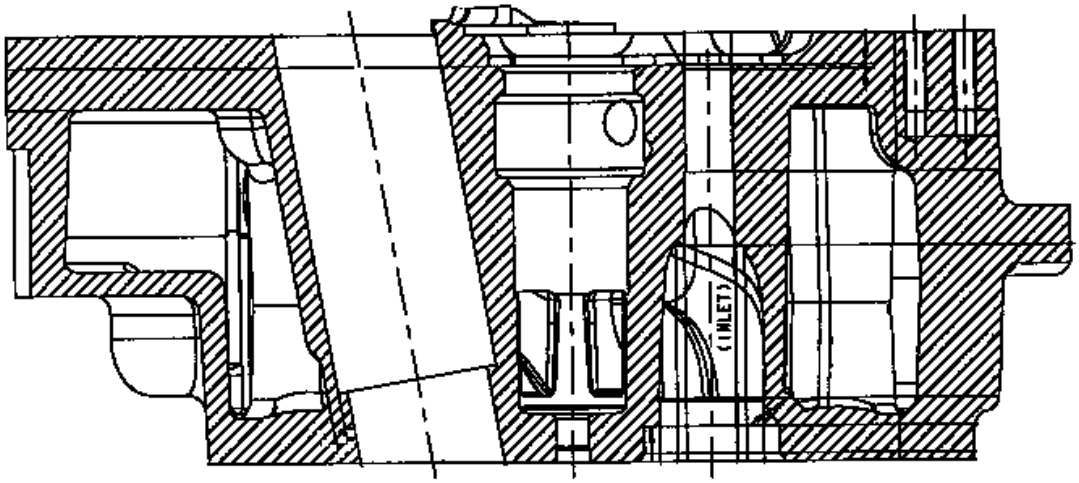

Figure 23. Side view cut of the optical cylinder head.

9.3 Endoscope

An endoscope was used to obtain optical access through the unmodified 4 valve cylinder head. The main imaging detector used with the endoscope was a PCO PixelFly CCD camera. The images acquired were subjected to two-colour analysis using the AVL VisioScope 1.1 software package in order to determine the distribution of temperature and soot in the cylinder.

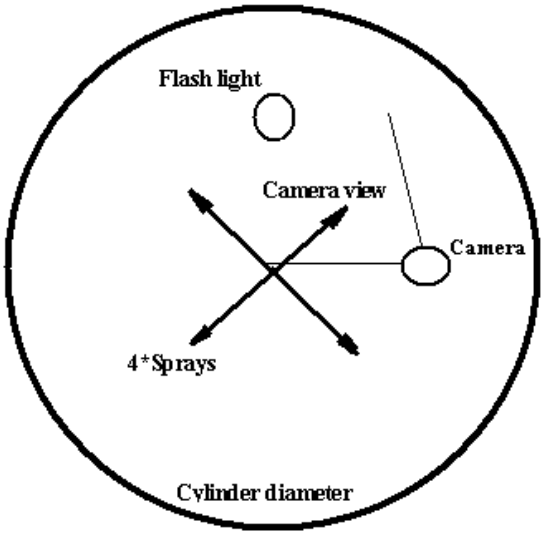

Figure 24. Schematic showing the position of the endoscope camera and the flash light within the cylinder when set up to capture images of one of the four sprays that propagate from the centre of the cylinder during engine operation.

10. Experimental equipment used in spray studies

Investigations were conducted to determine how cavitation and momentum affected various spray parameters as well as the ignition delay, flame structure and soot distribution for a real-size diesel nozzle under realistic diesel engine operating conditions. Experiments were performed in a high pressure, high temperature combustion rig to compare two different nozzles that had been manufactured using different degrees of hydro grinding (HG). In the context of diesel engine nozzles, the term hydro grinding refers to the process of forcing an abrasive fluid through nozzles with sharp inlet edges such that the sharp edges are worn. The process is continued until the desired flow rate is achieved.

A stainless steel vessel capable of handling air at 900 K and 10 MPa equipped with up to four quartz windows of 120 mm length and 40 mm width was used for the combustion studies. Compressed air was heated before entering the vessel. The flow velocity inside the vessel was between 10 and 15 cm/s, which can be considered quiescent relative to the velocity of the injected fuel. The vessel has a vertical hole at the top to accommodate the diesel injector. A common rail injection system was used to inject diesel fuel at 80 MPa through the injector via a vertical single-hole nozzle. The common rail injector was coupled to a control system that made it possible to adjust the injection duration and fuel pressure. Experiments were performed in air at 6 MPa and 830 K.

Two nozzles, one with 0 % hydro grinding (0.215 mm diameter) and another with 20 % hydro grinding (0.199 mm diameter), were selected for these experiments based on spray impingement measurements that showed them to have identical spray momentum profiles. A HYCAM-I camera was used to record the development of the spray over time at a rate of 8000 frames per second on negative film. A CCD camera coupled to the computer control unit was used to obtain images of the spray and the soot radiation from the flames in order to determine the soot concentration and flame temperature by means of two-colour method.

Three different measurement techniques were used with the high pressure and high temperature vessel:

1. DIRECT PHOTOGRAPHY BASED ON MIE SCATTERING – LIQUID PENETRATION

A CCD camera with an exposure time of 10 microseconds was coupled to a computer-controlled flash unit and used to image the scattered light from the liquid droplets of the injected fuel. This exposure time was short enough to "freeze" events and capture images of the spray pattern and penetration.

2. SCHLIEREN SYSTEM FOR VAPOUR PENETRATION

The Schlieren technique was used to visualize the fuel vapor flow. This method is based on measuring the deflection of light passing through the jet due to heterogeneities associated with density gradients that cause changes in the refractive index.

3. TWO COLOUR METHOD - FLAME TEMPERATURE AND SOOT CONCENTRATION

The intensity and wavelength distribution of the radiation emitted by the heated soot particles depend on their temperature. Matsui [63] has shown that by assuming the soot particles behave as gray bodies in terms of emissivity and comparing the intensities of their emissions at two different wavelengths, it is possible to estimate their temperature and the soot concentration. The distribution of the flame temperature and soot concentration was determined by analysing CCD images on a pixel-by-pixel basis using the Thermovision image analysis software package (AVL List GmbH).

11. Discription of each paper

Paper 1. The Effect of Elliptical Nozzle Holes on Combustion and Emission Formation in a Heavy Duty Diesel Engine, SAE 2000-01-1251,

The aim of the study presented in paper 1 was to determine how the use of non-circular nozzle holes would affect the emissions and fuel consumption of a diesel engine. Studies on gas jets have shown that the use of elliptical rather than circular nozzle holes can increase air entrainment into the jet. In some cases, this causes a phenomenon known as axis switching in which the jet spreading angle in the minor axis plane is greater than that in the major axis plane, as shown in figure 25. This could have significant effects on mixing processes [81,82]. Axis switching has also been observed in studies on liquid sprays generated by injection through elliptical holes into a gas [83].

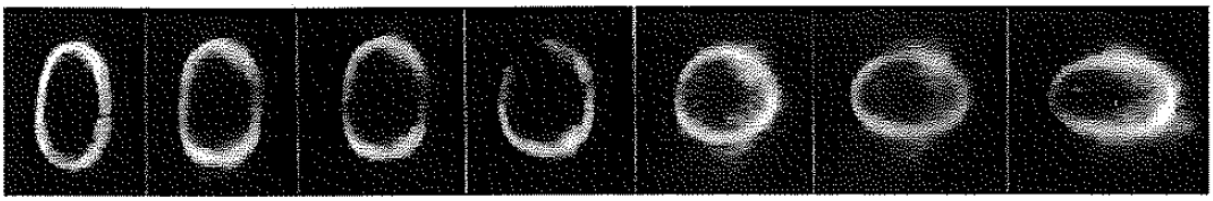

Figure 25. Axis switching as observed by Hussain & Husain [82].

Other experiments involving the injection of a liquid into a gas via non-circular nozzle holes produced sprays with a cone angle from the minor axis that was similar to that from the major axis in one case [84], and greater than that from the major axis in a different case [85]. Because increasing the degree of air entrainment could have beneficial effects on emissions, preliminary experiments were conducted at Chalmers using a passenger car diesel engine [86] and a single cylinder engine with optical access [87]. These studies revealed that the use of nozzles with elliptical holes reduced NOx emissions relative to those observed with circular holes. However, the elliptical holes did not reduce the emissions of particulate matter, carbon monoxide, or hydrocarbons, even though an increased level of air entrainment would be expected to reduce particle emissions. One of these investigations [86] was conducted using a small-bore engine, and it was suggested that spray wall effects may have affected the results obtained. To address this issue, new experiments were conducted using an engine with a larger piston bowl.

The experiments reported in Paper 1 were conducted using nozzles that had near-elliptical holes with an aspect ratio of approximately 2:1. For comparative purposes, experiments were also performed using an injector with circular nozzle holes and a similar hydraulic area. The elliptical holes where manufactured at Warsaw University of Technology and had no hydrogrinding. The circular reference nozzle was chosen from several production nozzles. Emissions measurements showed that the non-circular holes had higher smoke values but lower NOx values for given timings compared to the reference nozzle for both low and high loads. In addition, the non-circular holes yielded a better BSFC-NOx trade off at both low and high loads as shown in figure 26. The peak rate of heat release values for the non-circular holes were slightly lower than those for the circular holes. The smoke values for the non-circular holes were higher than those for the circular holes, and the anticipated reduction was never observed. In addition, the ignition delay observed with the non-circular nozzles was 0.5 CAD longer than that for the circular holes. Due to the improved BSFC-NOx trade off observed with the non-circular nozzles, it was decided that a second test should be conducted. Overall, the conclusion from the studies reported in Paper 1 was that it would be necessary to manufacture the non-circular nozzles more carefully, and that all nozzles being compared should be produced using the same grade of hydrogrinding. In addition, it was suggested that more care should be taken to ensure that all of the tested nozzle holes had identical spray hole cone angles. It was also concluded that the fuel flow should be tested at pressures that would be used in a real engine rather than by simply performing a 100 bar test. In addition, an optical cylinder head was designed and manufactured to enable investigations of the flame/wall interaction.

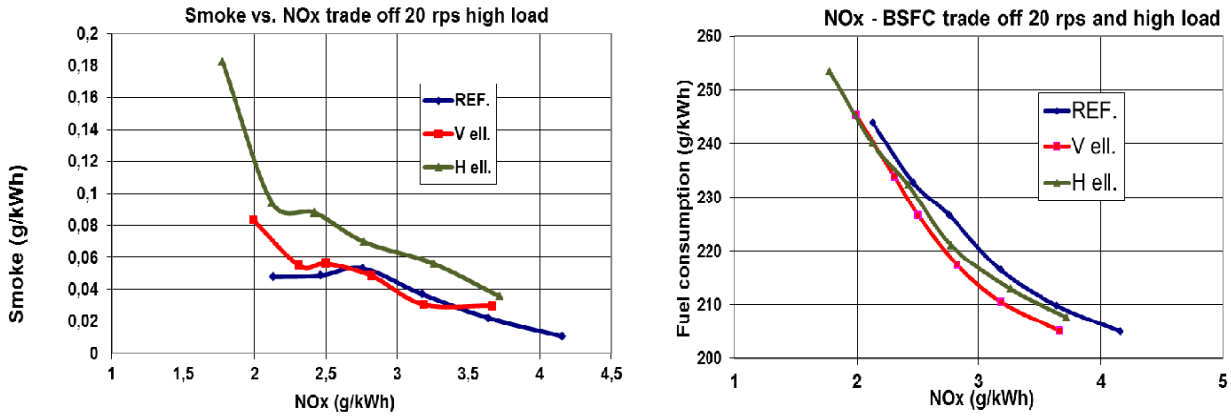

Figure 26. Smoke-NO_x and fuel consumption-NO_x trade off curves at 20 rps and high load. REF=circular reference. V and H ell.= Elliptical hole with major axis vertical resp. horizontal.

Paper 2. The effect of nozzle inlet conditions on fuel consumption and emissions of a heavy duty diesel engine, JSAE 2001-5345.

The nozzles used in Paper 1 differed in their grade of hydrogrinding and an investigation was conducted to determine how the grade of hydrogrinding applied to the nozzle affects the engine's emissions and fuel consumption. Some tests of this sort have been reported [43,78]. In addition, Pierpoint and Reitz [78] used nozzles with identical geometrical diameters and different discharge coefficients, which they compensated for by adjusting the injection pressure to achieve the same fuel injection rate in each case. Their results indicated that using nozzles that have not been subjected to hydrogrinding reduces smoke emissions but increases NOx emissions. This is inconsistent with the findings of Kampmann [43], who equalized the fuel flow through the different nozzles by varying the areas of the holes rather than the injection pressure. The engine tests reported in Paper 2 were conducted using two nozzles with circular holes and similar hydraulic areas. The "sharp" nozzle had no hydrogrinding but a slightly greater geometrical diameter to compensate for its lower discharge coefficient compared to the "round" nozzle having 20% hydrogrinding. Experiments were conducted at both low and high loads. It was found that the engine's fuel consumption decreased over time, and that a run-in time of 6 to 8 hours was required for it to stabilize. At low load, the fuel consumption fell by around 2% over the course of the run-in period when using the sharp nozzle, and about 1% for the round nozzle, compare 1st and 2nd in figure 27. In contrast to the case in Paper 1, there was no difference between the two nozzle types in terms of the resulting ignition delay.

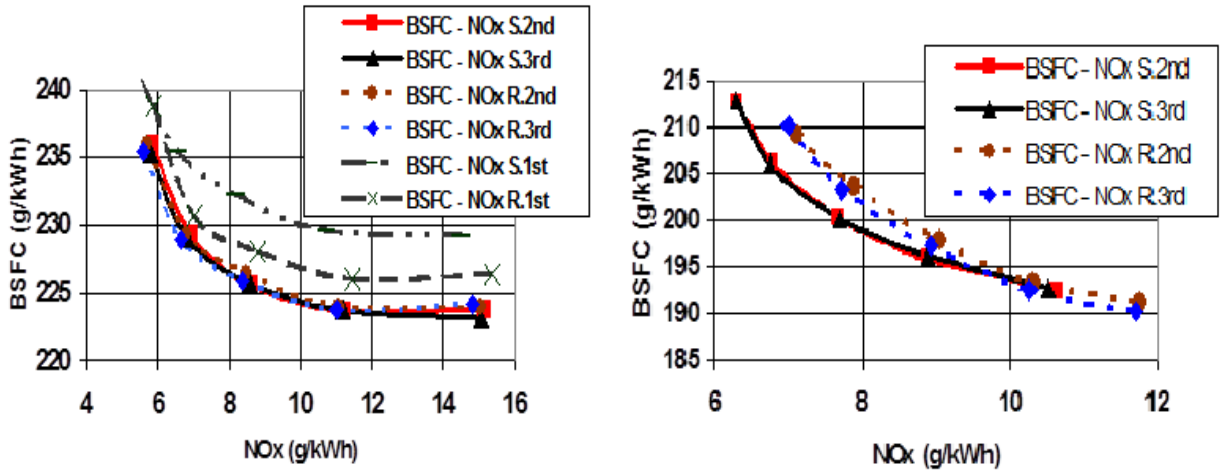

Figure 27. Fuel consumption – NO_x trade off curves at low load (left) and high load (right) when using the sharp and round nozzles. S=sharp inlet, R=round inlet.

The fuel consumption achieved using the round nozzle was lower than that for the sharp nozzle at the same injection timing at high load, see figure 27. The emissions measurements revealed that the round nozzle had a better smoke-NOx trade-off curve at low loads than the sharp nozzle because it produced lower smoke emissions but similar NOx emissions. The observation that the sharp nozzle produced higher smoke emissions contradicts those of Pierpoint and Reitz [78] but is consistent with Kampmann's findings [43].

The RoHR curves at high load revealed a distinct change in the RoHR for the sharp nozzle at about 1.5 ms or 10 CAD after the start of injection (figure 28). This pronounced change is believed to be due to the quenching or cooling of the flame when it hits the piston or is deflected upwards in the direction of the combustion chamber ceiling. It may also be a consequence of flame-to-flame interaction following the impact with the piston wall. Because this effect was not observed with the round nozzle, it was suggested that the sharp nozzle may produce a greater flame surface area. The sharp nozzle is more likely to cause cavitation and would therefore probably create a larger spray angle and a larger flame front area. The increased flame quenching would also explain the higher smoke and lower NO_x emissions achieved with the sharp nozzle.

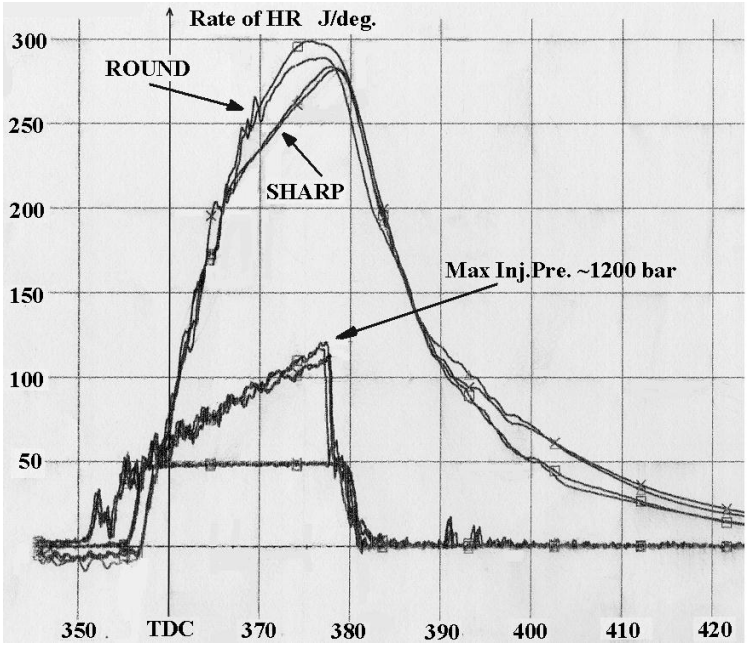

Figure 28. Rate of heat release at 20 rps and high load (300Nm) with the SOI at 356 CAD.

Paper 3. The Effect of Non-Circular Nozzle Holes on Combustion and Emission Formation in a Heavy Duty Diesel Engine, SAE 2002-01-2671

Paper 3 describes studies conducted using nozzles with both elliptical and slit-shaped holes. In addition, two orientations of the holes' major axes were considered – horizontal and vertical (see figure 29). The elliptical holes had an aspect ratio (AR) of about 2:1 while the slits had an aspect ratio of about 4:1. In addition, two standard production nozzles with fuel flows similar to those for the corresponding non-circular holes were used as sources of reference data. All of the studied nozzles were hydro grinded at Delphi, see Table 2.

Table 2. The degree of hydrogrinding applied to the non-circular nozzles (V2,H2,V4,H4) and the sizes of their holes relative to the reference nozzle.

Nozzle	Hydro grinding %	Average hole area in relation to reference
V2=2:1 vertical	23	1,05
H2=2:1 horizontal	26	0,97
V4=4:1 vertical	10	1,15
H4=4:1 horizontal	18	1,46

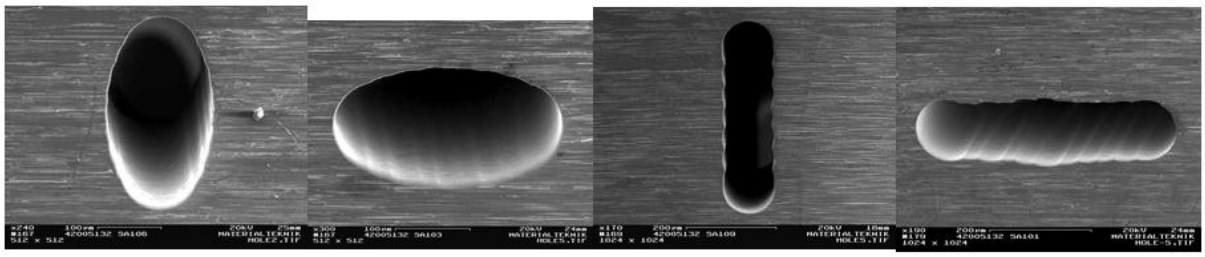

Figure 29. Selected images of the non-circular holes used in Paper 3 termed V2, H2, V4, H4.

In the low load experiments, the smoke-NOx and BSFC-NOx trade-off curves obtained using the nozzles with an aspect ratio of 2:1 differed only slightly from those for the reference nozzles. However, the reference nozzle curves (REF1) were consistently better than those for the elliptical nozzles, regardless of orientation.

At high loads, there were only very minor differences between the smoke/NO_x and BSFC/NO_x trade off curves for the different nozzles, as shown in figure 30. When using early injection timings, the non-circular holes had slightly lower NO_x levels whereas the non-circular holes produced slightly higher smoke levels with later injection timings.

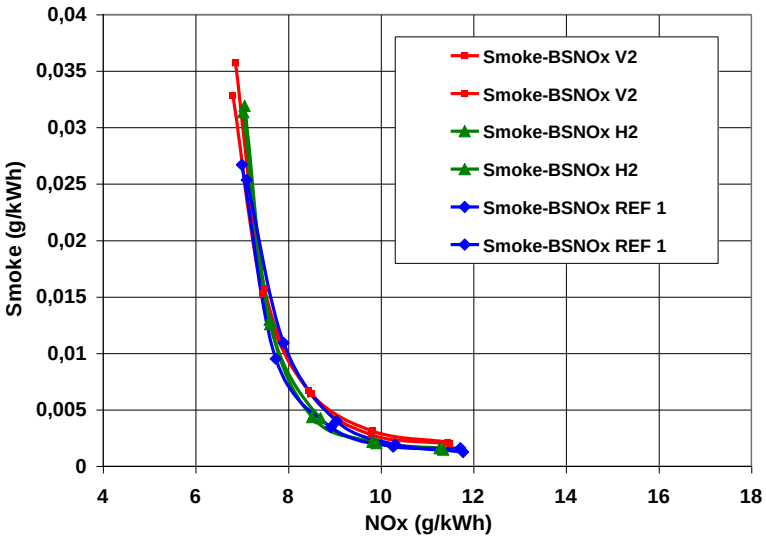

Figure 30. Smoke/NO_x trade-off curves for the reference nozzle and for the elliptical nozzles (V2 & H2) in the horizontal and vertical configurations at high load. Repeated timing swings.

The high-load RoHR curves for both non-circular holes with an AR of 2:1 had a pronounced deflection at about 10 CAD after SOI. This deflection was observed for SOI values of 350, 356 and 359 CAD; figure 31 shows the RoHR curve for an SOI at 359 CAD. Injection at 353 or 362 CAD yielded a deflection at 17 CAD after SOI.

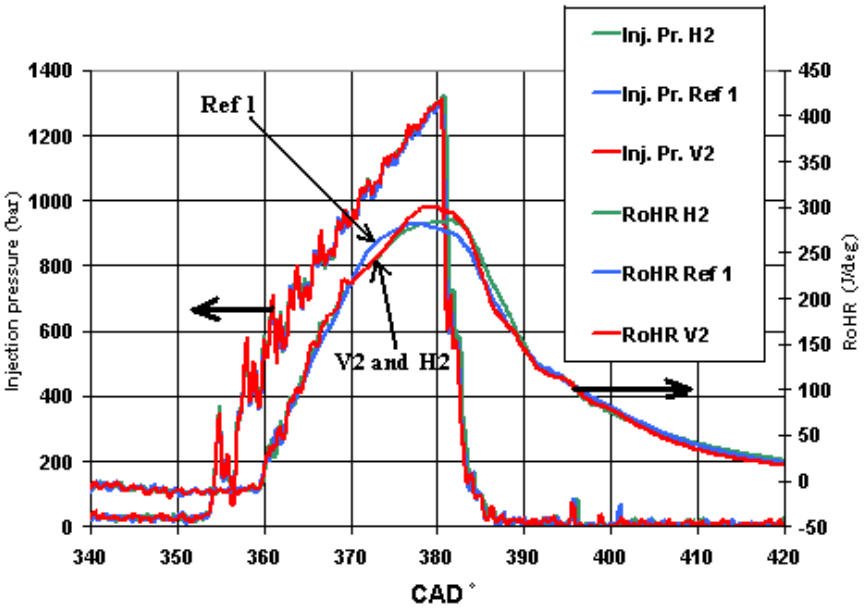

Figure 31. Injection pressure and rate of heat release (RoHR) curves generated using the AR 2 non-circular holes and the reference nozzle with an SOI at 359 CAD.

When using the AR4 nozzles, the horizontally-oriented H4 were so wide that they were made at two different heights. In addition, the flow values for the two AR4 nozzles differed slightly and were also slightly different to that for the first reference nozzle. A second reference nozzle, REF2, was therefore selected. The H4 nozzle produced substantially more smoke, less NOx and higher fuel consumption than both the V4 nozzle and the reference, at both low and high loads. Conversely, the differences between the results for the V4 and REF2 nozzles were relatively small. At low load, the V4 nozzle had slightly better smoke/NO_x and BSFC/NO_x trade-off curves, but the differences were small and the curves overlap. At high load, the situation is similar: the V4 nozzle generally produces more smoke and slightly higher fuel consumption but lower NO_x emissions for a given timing. However, the differences between the curves for the two nozzles are small, as shown in figure 32. As with the AR2 nozzle, the RoHR curve for the AR4 nozzle exhibited a pronounced deflection at about 9 to 11 CAD after SOI and the V4 nozzle had a slightly lower maximum RoHR and a marginally higher RoHR at the end of combustion compare with REF2. (see figure 33). In contrast to the results obtained in Paper 1, there were no differences between the nozzles in terms of the ignition delay for any of the compared cases.

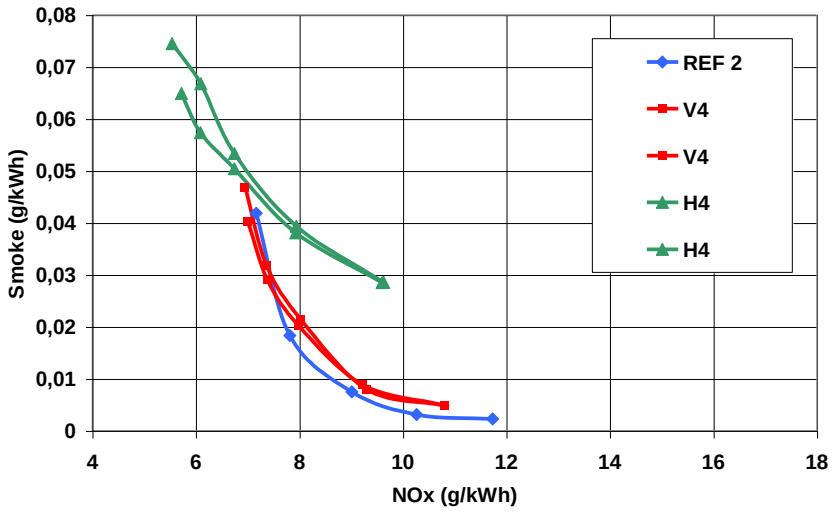

Figure 32. Smoke/NO_x trade-off curves for the aspect ratio 4 non-circular holes (V4 and H4) and reference nozzle REF2 at high load. Repeated timing swings.

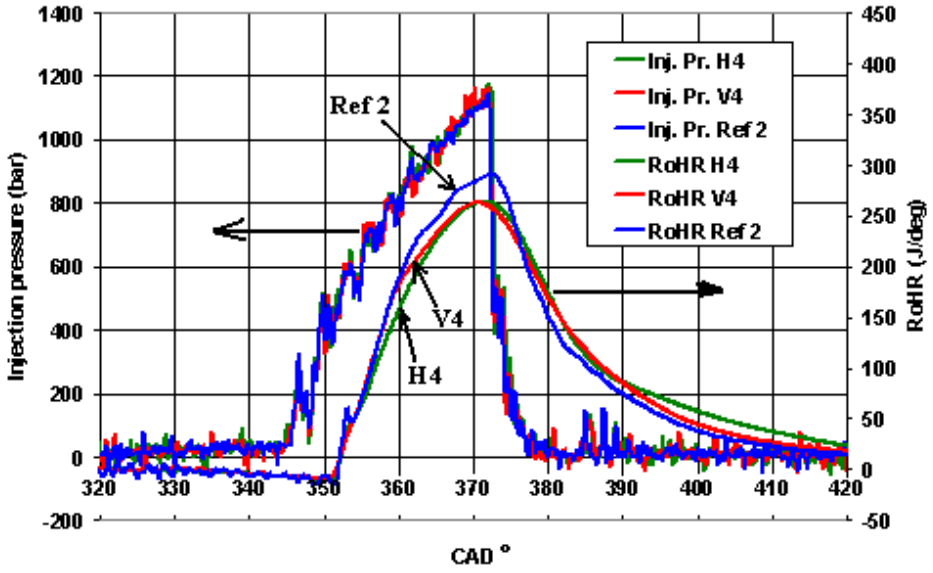

Figure 33. Injection pressure and rate of heat release (RoHR) curves for the aspect ratio 4 non-circular holes and reference nozzle REF 2 at SOI 350 CAD.

The anticipated increase in air entrainment for the non-circular holes was not confirmed by the emissions measurements since no significant reduction in smoke emissions was observed for either the AR2 or AR4 nozzles. This was true for the low load case, in which much of the fuel burns under premixed conditions, and also for the high load case with higher injection velocities. Interestingly, the difference in emissions and fuel consumption between the two reference nozzles, REF 1 and REF 2, was greater than that between the V4 nozzle and the REF2 reference nozzle. The optical cylinder head in figure 23 was used to take images of the light generated during combustion. Flame penetration was determined from the images and at 9-11 CAD after SOI it was found that this was approximately when the flame made contact with the piston bowl, see figure 34. The images were recorded during the low load experiments, but they are also believed to be representative of the high load case, in which similar deflections of the RoHR curves were observed. The fuel pressure build up is the same at low and high load, and the fuel injection duration in the low load case is on the order of 7 CAD long. Therefor the flame could possibly achieve the same length of penetration into the cylinder at 9 CAD after SOI also in the high load case, even though the chamber pressure would be higher**.** When the fuel injection was timed at 353 or 362 CAD, the deflection in RoHR curves occurred at 17 CAD after SOI for the AR2 non-circular nozzles. These deflections are probably due to contact between adjacent flames or between flames and the cylinder head. Figure 35 shows the images acquired with the camera at 15, 17 and 18 CAD after SOI for an injection timing of 350 CAD.

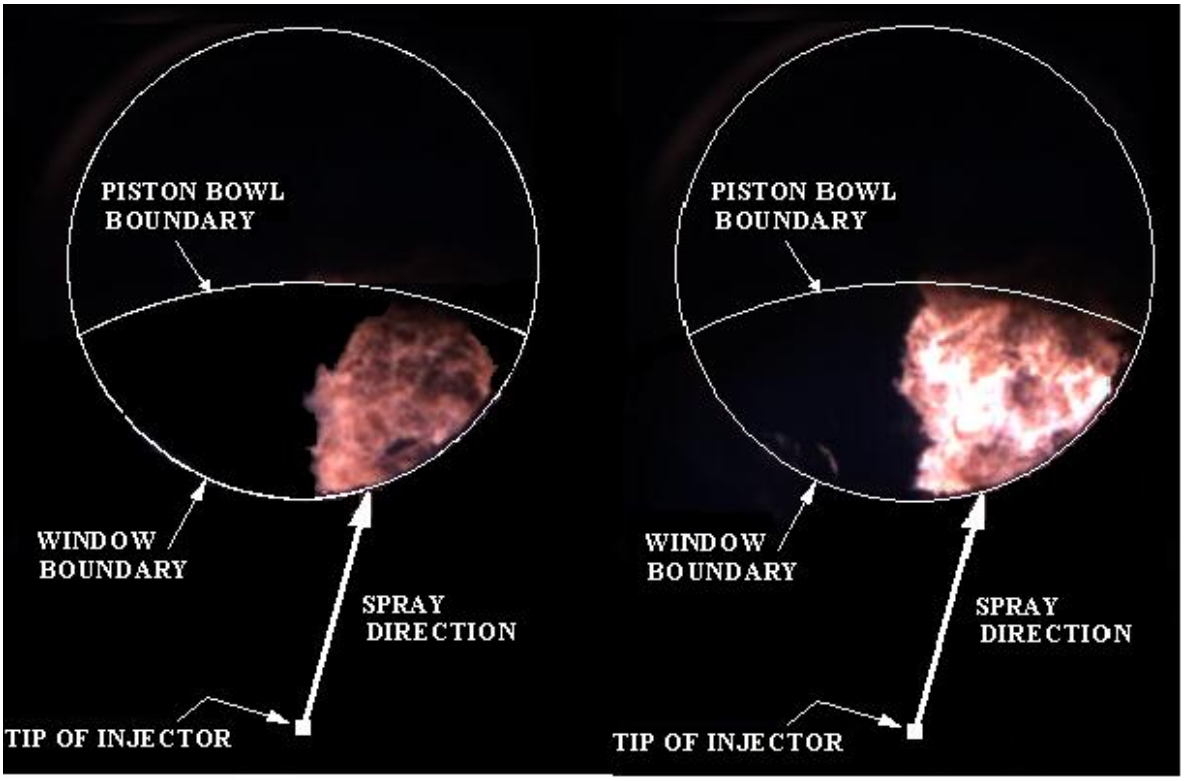

Figure 34. Photos showing natural radiation generated in the combustion chamber, taken from the chamber ceiling. The engine was operated at 20 rps and 75 Nm with SOI at 356 CAD. The left-hand picture was taken at 9 CAD after SOI, the right-hand picture at 11 CAD after SOI.

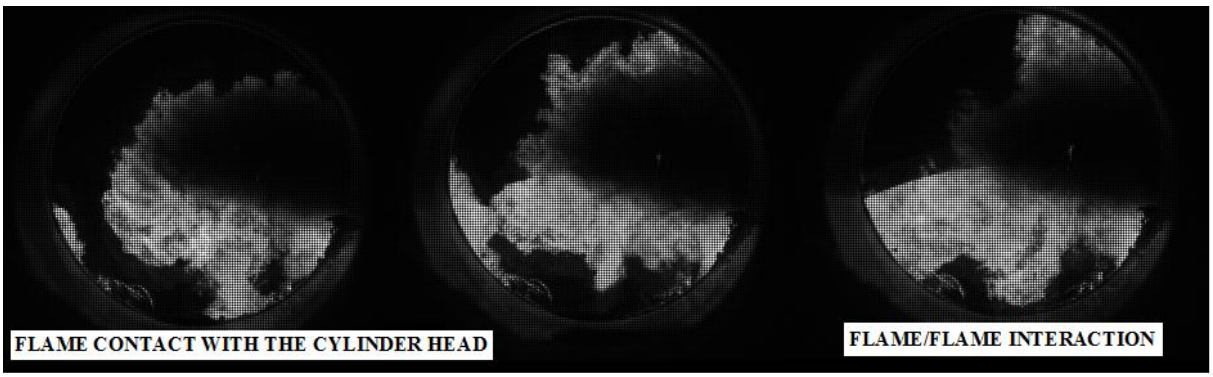

Figure 35. Photographs showing natural light flame propagation at 15, 17 and 18 CAD after SOI in a low load experiment with SOI at 350 CAD.

It was concluded that the hole shape does not significantly affect emissions or fuel consumption and that the piston bowl dimensions have an important role. Also, two almost identical nozzles, REF1 and REF2, had rather different effects on emissions and fuel consumption that in some cases greatly exceeded the differences between circular and non-circular holes. These two findings suggest that nozzle hole shape in itself does not strongly affect emissions and fuel consumption, and that it is more important to focus on other factors.

Paper 4. Combustion Characteristics of Diesel Sprays From Equivalent Nozzles With Sharp And Rounded Inlet Geometries. Combustion Science and Technology, 176 (6), 1015-1032. 2003.

The experiments reported in Paper 4 were conducted in a chamber at a pressure of 6 MPa and a temperature of 830 K. These values were selected to represent typical engine operating conditions. A common rail injection system was used to inject diesel fuel at 80 MPa. The aim was to investigate the spray and flame formed by injection through a single-hole circular nozzle. Two different nozzles were used; both had vertically oriented axisymmetric holes but with different diameters and hole inlets. Specifically, one had a sharp-edged inlet hole while the other had a rounded edge. Several authors [9, 12, 33, 42] have argued that cavitation has significant effects on atomization. However, this is somewhat controversial, and Baddock [22] did not observe any relationship between cavitation and spray atomization in a full-size nozzle under transient conditions.

Several different measurements were made to characterize the sprays and flames generated using each nozzle. Impingement measurements acquired with a pressure transducer showed that the two nozzles produced sprays with the same momentum but had different injection velocities, discharge coefficients, and calculated losses of kinetic energy (see figure 36). The nozzle with the rounded inlet had higher injection velocity and discharge coefficient but lost less kinetic energy to turbulence. The spray was photographed with a CCD camera and the images were converted into binary format to trace the edges of the spray and measure the spray angle and spray penetration. The two nozzles were found to produce spray angles that differed by only around 1 degree, which is consistent with the findings of Baddock [22]. The differences between the two nozzles in terms of spray penetration were similarly modest. The 2D flame images captured using the CCD camera were assumed to exhibit rotational symmetry and processed using a computer program. Each nozzle was photographed at 8 different time points; fifty images were acquired for each time point and averaged for analysis. The rate of flame development was found to be slightly higher for the nozzle with the rounded inlet, as shown in figure 37.

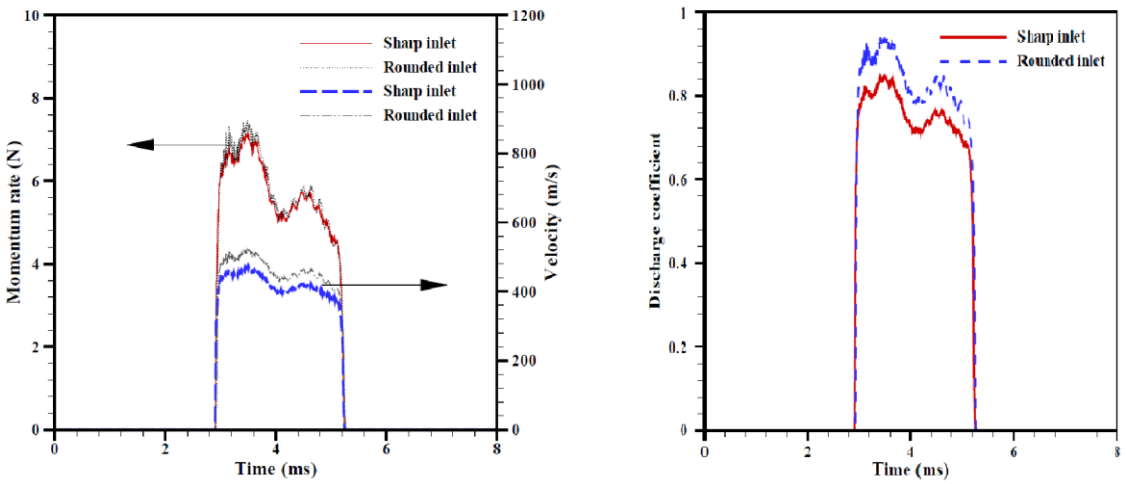

Figure 36. Transient fuel jet momentum and injection velocity profiles (left) and variation in the discharge coefficient over time (right) for the sharp and round nozzle inlets.

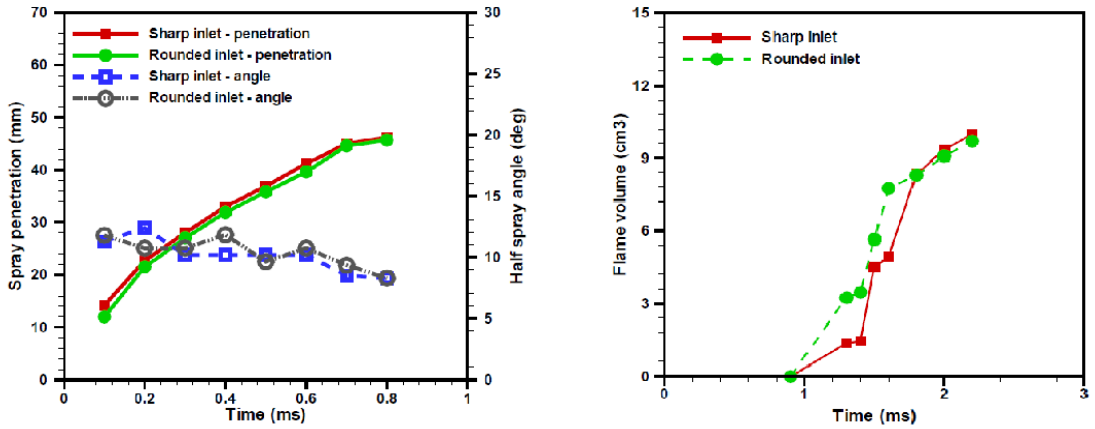

Figure 37. Spray penetration and spray angle during the ignition delay (left) and the flame volume at various time points after start of ignition (right) for sharp and round inlet nozzles.

Ignition was found to be approximately 2.4 to 2.7 mm downstream of the nozzle hole exit at about 1 ms after SOI for both nozzles. There were no clear global differences between the flames produced with the sharp and rounded nozzles. A rapid burnout of the trailing edge was observed. This phenomenon was explained by Musculus et al. in 2009, who argued that the abrupt EOI creates an entrainment wave that propagates at twice the initial jet penetration rate, increasing the entrainment of the ambient gases several times over. Once this entrainment wave reaches the head of the jet, the jet penetration rate is reduced [64, 65]. It was concluded that in the absence of obstacles, diesel spray combustion is primarily governed by the momentum of the spray, and the internal nozzle flow structure does not matter as long as it does not change the fuel jet's momentum.

Paper 5. Comparing Different Grades of Hydro Grinded Nozzles in a Heavy Duty Diesel Engine, SAE 2003-01-3420

Paper 5 presents results from three different sets of experiments. The first experiment is using a collection of nozzles that had been subjected to different grades of hydrogrinding, all with a 153 degree spray hole cone angle. With the same flow rate, but increasing fuel injection velocity due to differences in discharge coefficient and hole diameters, the objective was to see the effect of continuous changing spray momentum and increasing air entrainment.

A second set of experiments was conducted using nozzles prepared with 20% and 50% hydrogrinding and a 155 degree spray hole cone angle. The increased spray hole cone angle relative to that used in the first set of experiments should change the contact area between the flame and piston wall or the cylinder head relative to that seen in the first set of experiments. A 155 degree spray hole cone angle was selected.

The final set of experiments was performed using nozzles with the same specifications as those used in the second set, but with four holes rather than six. In these experiments, an endoscope was used to record the combustion event and 2 colour analyses to determine the soot concentration and temperature within the cylinder. The images were recorded with a cycle to cycle variation and 5 images were averaged for each crank angle. The recorded interval span was 50 crank angles including the majority of the combustion phase. Calculated values were averaged in the AVL Visio Scope creating a sequence of 50 images. Three sequences per nozzle were then averaged so that 15 images was representing each crank angle degree. The sequences were converted into gray scale and an in-house Matlab program was used to calculate the percentage of the total flame area above a certain threshold value for the temperatures and soot levels. The results of the two colour analyses were then compared to the engine's emissions. Figure 24 provides a schematic view of the endoscope setup.

Paper 5 results – The effects of varying the degree of hydrogrinding in nozzles with a spray hole cone angle of 153°

The amount of smoke produced declined continuously as the degree of hydrogrinding increased for both low and high loads. At low loads, the smoke level from the 35% nozzle was almost constant over the whole timing swing and did not increase at late timings as it did

with the other nozzles (figure 38). NOx emissions increased with increased levels of hydro grinding at both high and low load, but the smoke-NOx emission trade off curves generally became more favourable as the degree of hydrogrinding increased.

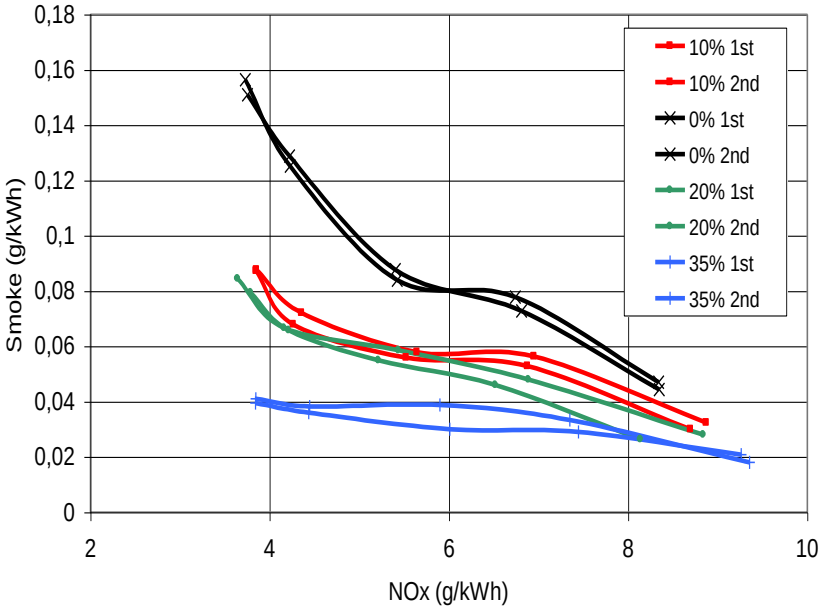

Figure 38. Smoke/NO_x emissions trade off curves for nozzles with 0% to 35% hydrogrinding at 20 rps and low load. Repeated timing swings.

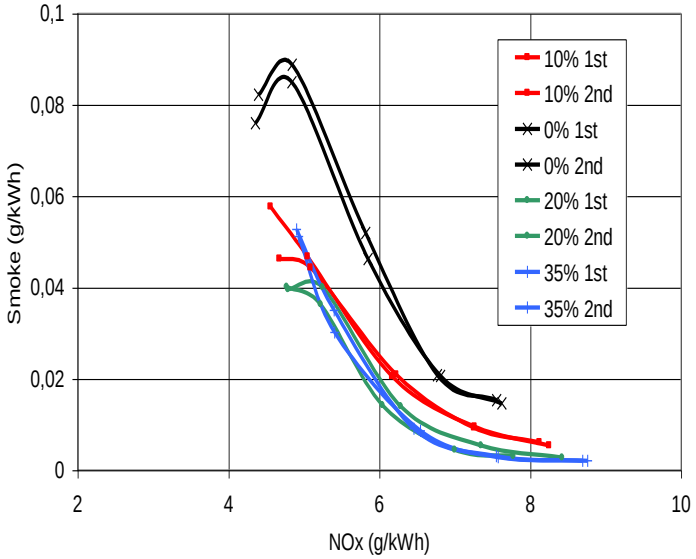

Figure 39. Smoke/NO_x emissions trade-off curves for nozzles with 0 to 35% hydro grinding at 20 rps and high load. Repeated timing swings.

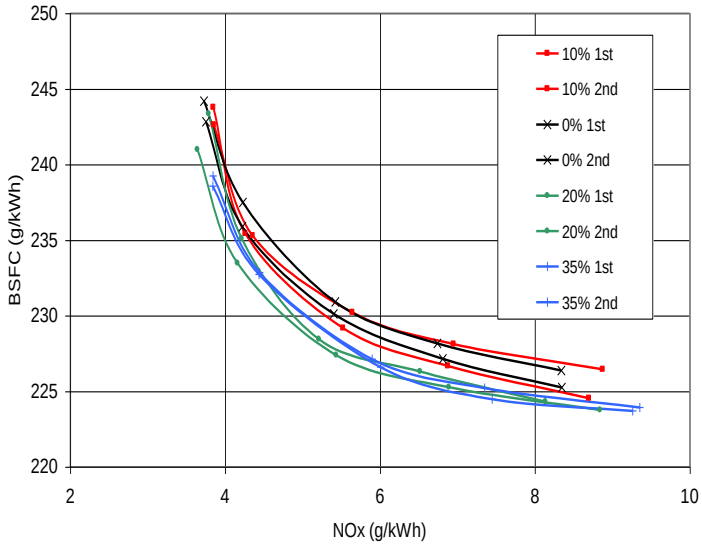

Figure 40. Fuel consumption/NO_x emissions trade-off curves for nozzles with 0 to 35% hydrogrinding at 20 rps and low load. Repeated timing swings.

The trade-off between fuel consumption and NO_x is also improved as the degree of hydrogrinding increased at low load, see figure 40, but no clear trend was observed under high load conditions, see figure 41. Possibly, the run-in time may have been too short for the 0 and 10 % nozzles under the low load conditions, since the first BSFC measurements for the 0 and 10% nozzles were around 1 g/kWh higher than the following second measurements.

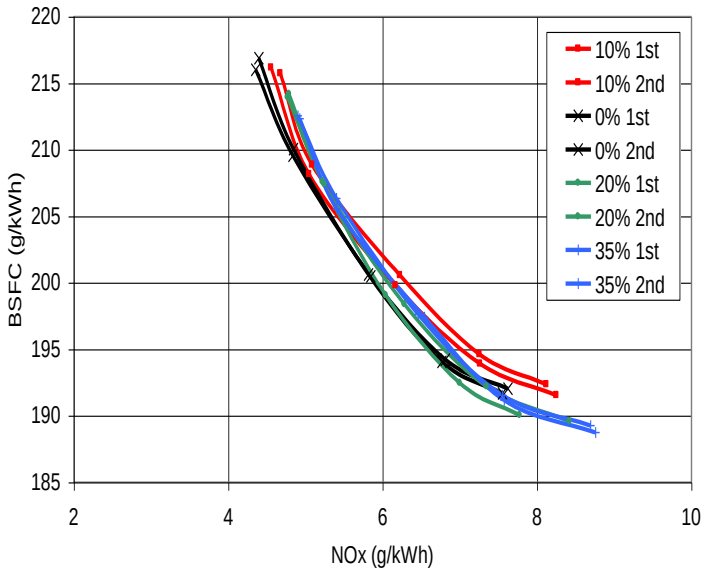

Figure 41. Fuel consumption/NO_x emissions trade-off curves for nozzles with 0 to 35% hydrogrinding at 20 rps and high load. Repeated timing swings.

In figures 42 and 43 the fuel consumption as a function of SOI is presented for both loads. Fuel consumption smoothly decreased with increased grade of hydrogrinding. This may be due to the higher combustion temperatures generated by such nozzles. In Paper 2, the RoHR curves for nozzles with no hydrogrinding exhibited a pronounced deflection under high load conditions. No such deflection was observed in these experiments for any nozzle at any load.

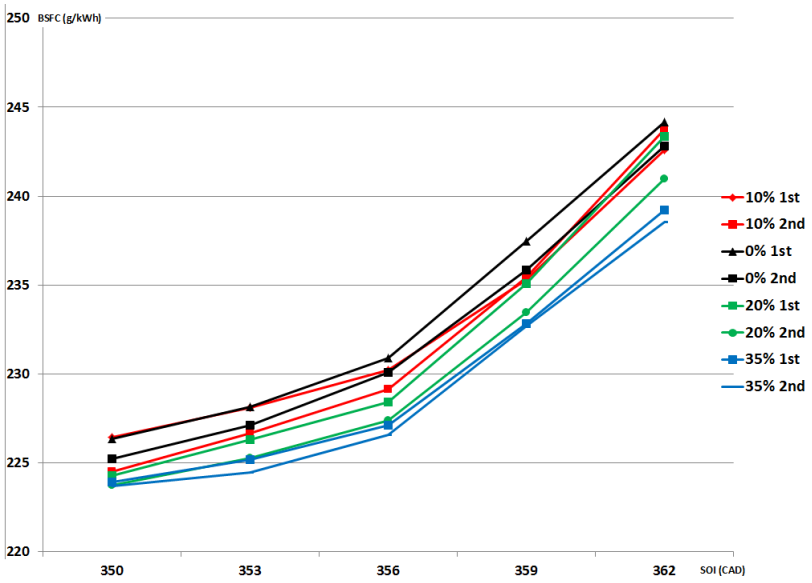

Figure 42. Fuel consumption as a function of the fuel injection timing at 20 rps and low load for nozzles with 0 to 35% hydrogrinding. Repeated timing swings.

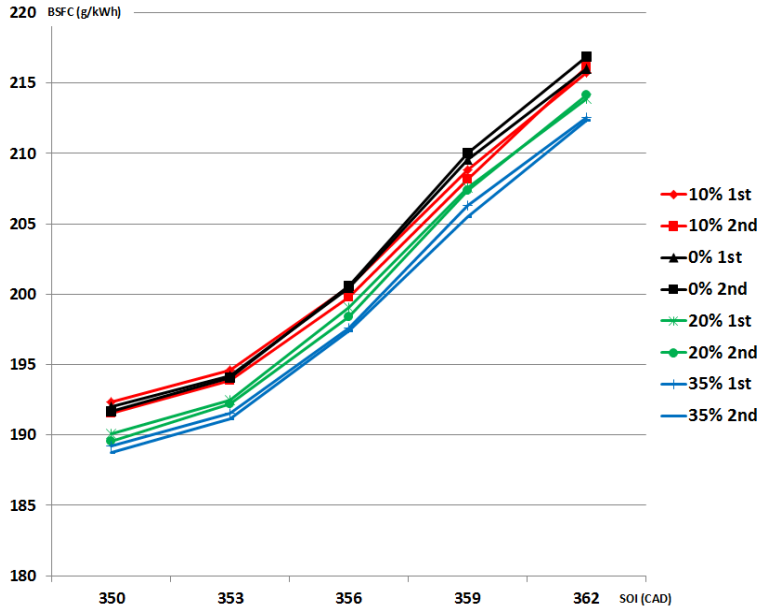

Figure 43. Fuel consumption as a function of the fuel injection timing at 20 rps and high load for nozzles with 0 to 35% hydrogrinding. Repeated timing swings.

Paper 5 results – The effects of varying the degree of hydrogrinding in nozzles with a spray hole cone angle of 155°

Under low load conditions, the nozzle with 50 % hydrogrinding produced lower smoke emissions but slightly higher NO_x levels than the 20% nozzle, giving a better overall smoke-NO_x trade-off curve (see figure 44). Some conditioning problems were encountered with the fuel consumption measurement equipment. Specifically, the finding that the 20% nozzle produced just under 6 g/kWh NO_x and 222 g/kWh BSFC at low load is probably erroneous because the fuel consumption normally decreases as NO_x emissions increases, see figure 45.

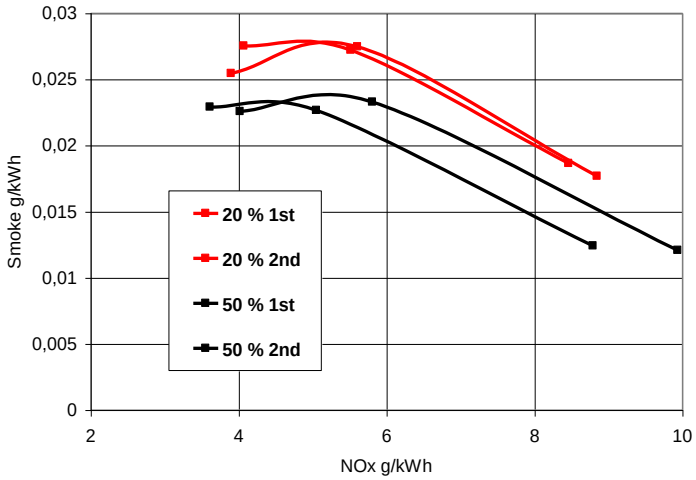

Figure 44. Smoke/NO_x emissions trade off curve for the 20 and 50 % hydro grinding nozzles at 20 rps and low load. Repeated timing swings.

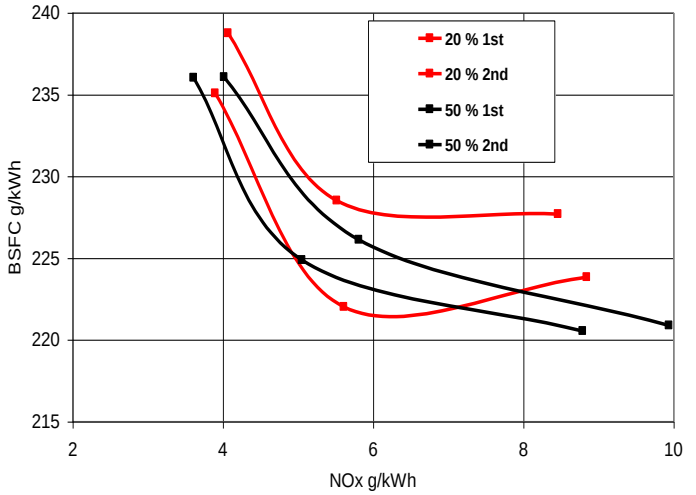

Figure 45. Fuel consumption/NO_x emissions trade-off curves for the 20 and 50 % hydro grinding nozzles at 20 rps and low load. Repeated timing swings.

At high load, there were no significant differences between the 20 and 50 % nozzles for any given timing or in any of the studied trade off curves. The correlation between reduction of fuel consumption and the degree of hydrogrinding that was observed in the first set of experiments of Paper 5 was not as obvious in the second set of experiments from Paper 5.

The results obtained under high load conditions in the first and second sets of experiments clearly show how strongly the spray hole cone angle and the flame/wall interaction affect the combustion process. Specifically, increasing the spray hole cone angle from 153° (as in the first set of experiments) to 155° (as in the second set) halved the engine's smoke emissions and reduced its NO_x emissions by 1 g/kWh over the whole timing sweep (see figure 46). This change also significantly reduced the engine's fuel consumption over the studied timings, as shown in figure 47. For Test2 20 and 50 % SOI was 350, 356 and 362 CAD. For Test1 35% SOI was 350, 353, 356, 359 and 362 CAD, so all curves are within the same SOI span.

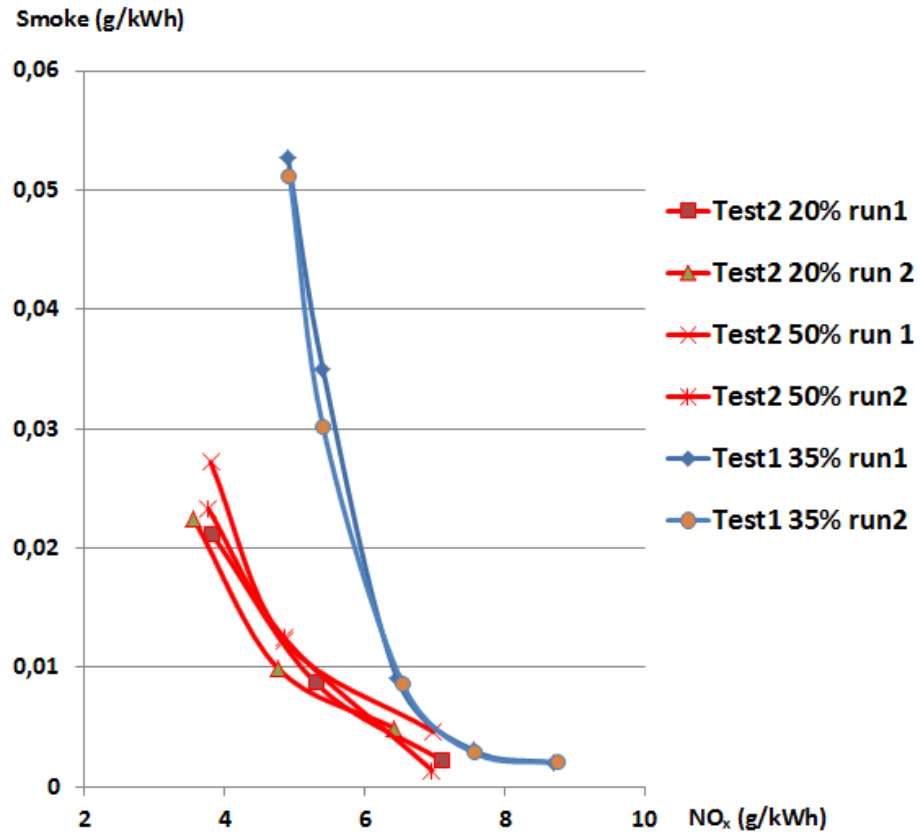

Figure 46. Smoke/NO_x emissions trade off curves for nozzles with spray hole cone angles of 153° (35% hydrogrinding) and 155° (20 and 50 % hydrogrinding) at 20 rps and high load. Repeated timing swings.

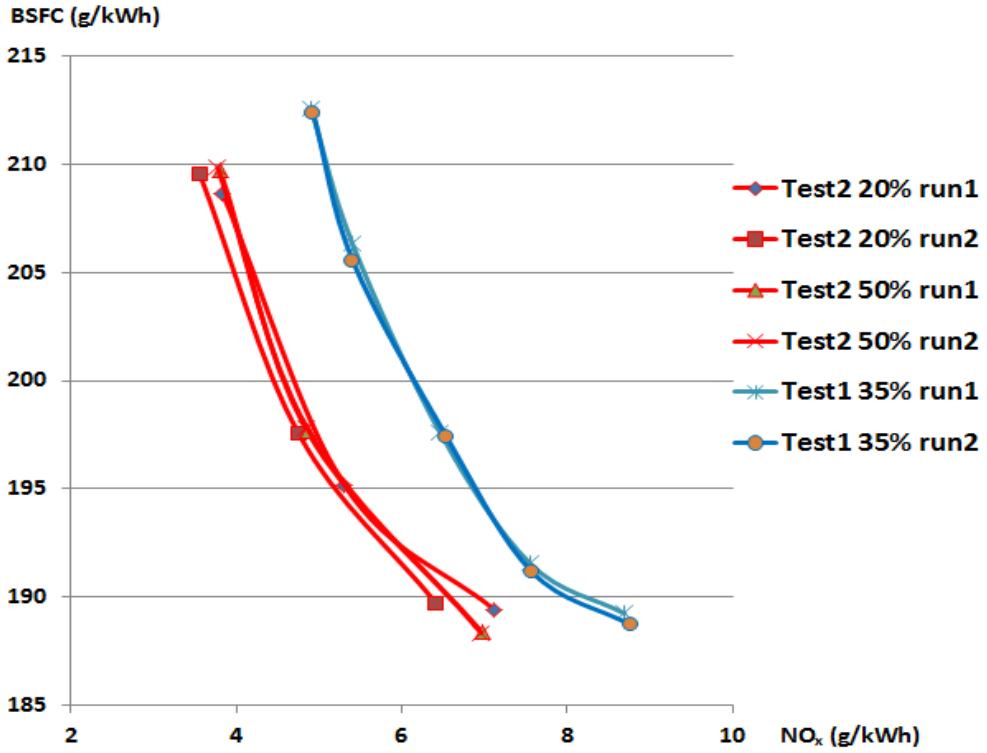

Figure 47. Fuel consumption/NO_x emissions trade off curves for nozzles with spray hole cone angles of 153° (35% hydrogrinding) and 155° (20 and 50 % hydrogrinding) at 20 rps and high load. Repeated timing swings.

Paper 5 results – Optical imaging of the combustion process using nozzles with different degrees of hydrogrinding

The third set of experiments demonstrated that the nozzle with 50% hydrogrinding produced a flame with a larger surface area above 2600 K than the 20 % nozzle (see figure 48). It was also determined that the 50 % nozzle produced a smaller flame area with high soot content (see figure 49). For both nozzles, the soot content peaked one CAD before the maximum temperature occurred. Because the soot concentration is depending on injected fuel rate, so is also the diffusion flame temperature. The third set of experiments also confirmed that the 50 % nozzle emits less smoke but more NO_x than the 20% nozzle. In Figure 50 examples of images with natural flame radiation, calculated soot concentration and the percentage of the flame with a temperature above 2200 K are shown.

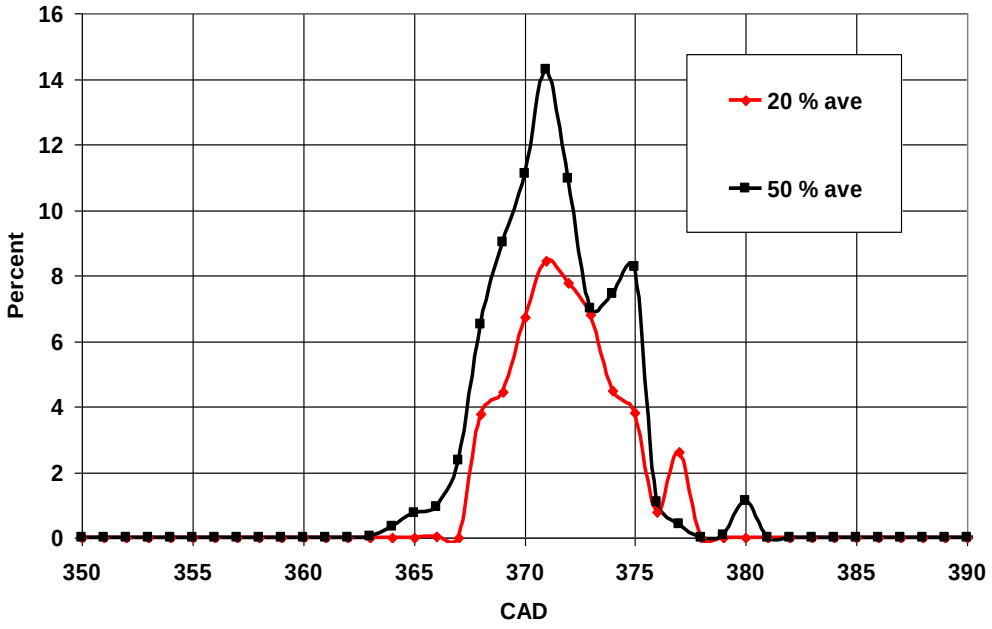

Figure 48. Percentage of the flame with a temperature above 2600 K for the 20 and 50 % hydro-grinded nozzles at low load with SOI at 350 CAD.

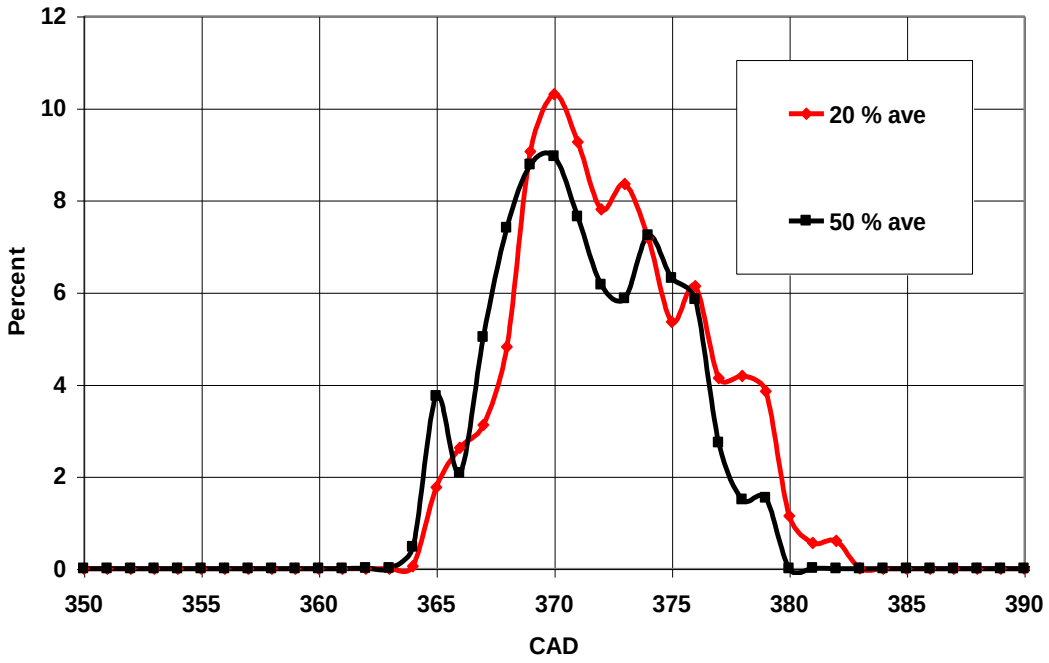

Figure 49. Percentage of the flame with a soot factor of more than KL 10 for the 20 and 50 % hydro-grinded nozzles at low load with SOI at 350 CAD.

It is believed that the difference in air entrainment and turbulent mixing is the reasons for the differences in the results in test 3. These findings resemble those reported in 2006 by Miers and Ciatti [73], based on a comparison of a straight-holed nozzle with 7% hydro-erosion and a conical nozzle with 17% hydro-erosion, but without providing any explanation for their results. Similar comparisons of engine emissions measurements with 2 colour pyrometry data and calculations of the percentage of the flame area that exceeds some threshold value have been reported in other contexts [75,76].

The results in Paper 5 demonstrate that increasing the degree of hydrogrinding caused a continuous decrease in smoke emissions and fuel consumption under both low and high load in the first set of experiments but not the second. While these decreases were accompanied by increased NO_x emissions, the overall trade-off remained favourable, especially at low loads. High turbulence and increased cavitation in the nozzle flow do not seem to have beneficial effects on emissions or fuel consumption. Comparing results from Test1 and Test2 demonstrated the strong effect of flame-wall interactions and the importance of piston bowl optimization. The two-colour pyrometry analyses indicated that the increased air entrainment and more intense mixing achieved by increasing the injection velocity will produce a flame with a comparatively large high-temperature area and relatively low soot concentrations. The differences observed using the two-colour method were small but consistent with the emissions measurements obtained in the engine tests. Our findings are consistent with those of Kampmann *et al.* [43], who also observed increased NO_x emissions and reduced smoke emissions along with a reduced duration of soot glow.

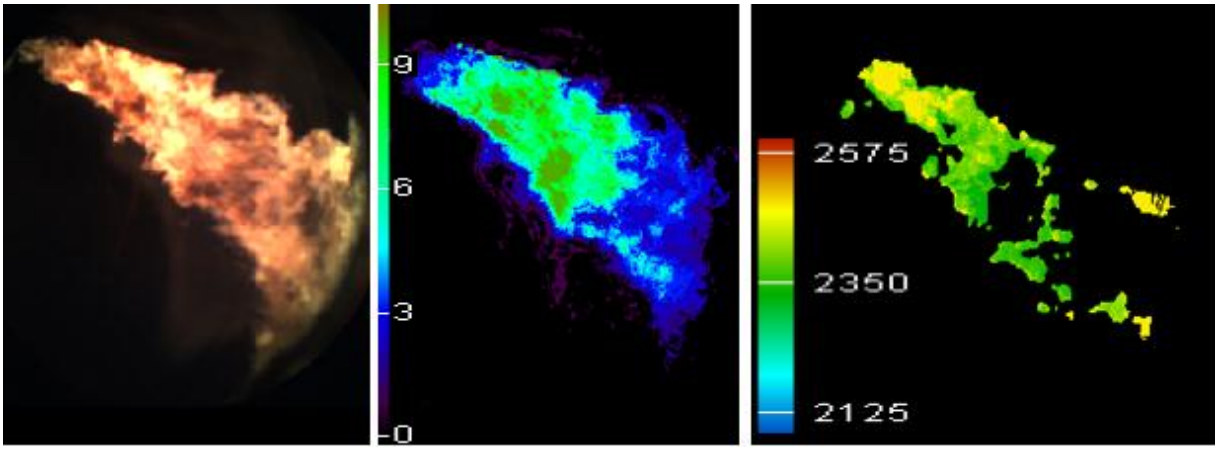

Flame radiation Soot concentration - KL Temperature above 2200 K

Figure 50. Representative images showing the natural flame radiation, calculated soot concentration (KL-factor) and calculated flame temperature during a typical experimental run

12. Conclusions

The key conclusions from these studies are:

- The anticipated reduction in smoke emission because of increased air entrainment for the non-circular holes compared with standard circular holes was not measured in the engine experiments. Instead smoke emissions increased with the non-circular holes. A distinct change in rate of heat release for the non-circular holes coincides with the point in time when the flame is observed to make contact with the piston bowl. The non-circular holes have a relatively larger hole area that will create a larger flame front areas that is quenched when impinging on piston bowl wall and cylinder head and also possible flame/flame interaction. The quenching will reduce the combustion intensity and more soot will survive the oxidation process. The larger hole area for the non-circular holes reduces the mean injection velocity and probably also the air entrainment. With lower injection velocity less energy can create small scale turbulence for the late oxidation process. Lower NO_x emissions were measured with non-circular holes and the NO_x – smoke and NO_x – fuel consumption trade off was similar as the circular reference nozzles.

- Increased spray cone angle due to increase in cavitation and turbulence in the nozzle hole will result in larger flame front area and lower injection velocity. Results from engine tests show that with a nozzle having no hydro grinding and therefore more cavitation, the rate of heat release is reduced more when the flame front area is impinging on piston bowl wall and cylinder head and also possible flame/flame interaction. With lower injection velocity, the amount of kinetic energy available to create small-scale turbulence during the late oxidation process decreases, reducing the scope for soot oxidation.

- Increasing the degree of hydrogrinding applied to the nozzle holes reduces smoke emissions at both low and high loads. The decrease in smoke emissions is due to increased air entrainment into the spray, which will reduce the formation of soot in the flame. Also, with a smaller spray cone angle the extent of the flame front area that is quenched following impingement on the piston bowl is reduced and possible also on the cylinder head as well as during potential flame/flame interactions. Increased levels

of hydrogrinding also reduce smoke emission by increasing the injection velocity, which increases the turbulence in the late oxidation phase and thereby provides more opportunities for soot oxidation. Two-colour pyrometric analyses of in-cylinder images demonstrated that increased hydrogrinding of the nozzle produces hotter flames with lower soot levels for the same injected fuel rate, injection timing and injection duration. The higher average flame temperature was consistent with measured engine-out NO_x emissions and was attributed to an increase in the diffusion flame temperature. The higher diffusion flame temperature was suggested to be due to increased air entrainment and also higher turbulence due to the higher injection velocities achieved when using nozzles with higher degrees of hydrogrinding. Increased degree of hydrogrinding can also reduce fuel consumption for a given timing. The reason is believed to be due to higher combustion temperatures. Increasing the degree of hydrogrinding applied to the nozzle yielded more favourable NO_x – smoke and NO_x – fuel consumption trade off curves despite increasing the engine's NO_x emissions.

- The effects of using non-circular holes and varying the degree of hydrogrinding had much less pronounced effects on the engine's emissions and fuel consumption trade-off curves than those caused by a change of 2 degrees in the spray hole cone angle (umbrella angle) with standard circular nozzle holes. It is therefore very important to match the nozzle's parameters to the properties of the piston when aiming to optimize emissions and fuel consumption.

- Because small fuel droplets are rapidly formed and vaporized in the engine, there is also a rapid transfer of momentum from the liquid to the gas phase. In this respect, diesel spray combustion is similar to gas combustion and is little affected by changes in the nozzle flow; instead, the combustion process is primarily governed by the jet's momentum. The internal nozzle flow is only significant if it changes the jet's momentum or distribution in time and space.

13. References

[1] http://www.bp.com/, 2013

[2] NUTEK, B 1992:4 “Dieselmotorn och dess utvecklingspotential. ISSN 1102-2566, ISBN 91-38-12743-1, 1992.

[3] Coal conversion technology, C.Y. Wen and E. Stanley Lee, Addison-Wesley Publishing Company, Inc., 1979.

[4] Heywood, J.B., “Internal Combustion Engine Fundamentals” McGraw-Hill, Inc. ISBN 0-07-100499-8, 1988

[5] Eismark J. et al., ”Role of late soot oxidation for low emission combustion in a diffusion controlled, high EGR, heavy duty diesel engine. SAE 2009-01-2813.

[6] Blessing, M., “Untersuchung und Charakterisierung von Zerstäubung, Strahlausbreitung und Gemischbildung aktueller Dieseldirekteinspritzsysteme”, Doktors Abhandlung, Universität Stuttgart, 2004.

[7] Ruiz, A.J., “A few useful relations for cavitating orifices”. In ICLASS’91, 1991.

[8] Payri, F. et al. “A contribution to the understanding of cavitation effects in Diesel injector nozzles through a combined experimental and computational investigation”. Computers and Fluids 58 (2012) 88-101. Elsevier

[9] Bergwerk, W., ”Flow pattern in diesel nozzle spray holes”, Proceedings of the Institution of Meachanical Engineers, Vol. 173, No. 25, pp. 655-660, 1959.

[10] Reitz R. D. and Bracco F. V., ”Mechanism of atomization of a liquid jet”, Phys. Fluids, Vol. 25, pp. 1730-1742, 1982.

[11] Hiroyasu, H., Arai, M., and Shimizu, M., ”Break-up length of liquid jet and internal flow in a nozzle”, ICLASS-91, Gaithersburg, pp. 275-282,1991.

[12] Hiroyasu, H., ”Spray break-up mechanisms from the hole-type nozzle and its applications”, Atomization and sprays, Vol. 10, No.3-5, pp.511-527, 2000.

[13] Soteriou, C., Andrews, R. and Smith, M., ”Further studies of cavitation and atomization in diesel injection”, SAE Paper 1999-01-1486, 1999.

[14] Badock, C., et al. 1997 ”Fundamental study of the influence of cavitation on the internal flow and atomization of diesel sprays”. In: Proceedings of ILASS –97, Florence, Italy, pp. 53-59.

[15] Kim, J-H., Nishida, K., Yoshizaki, T. and Hiroyasu, H., ”Characterization of flows in the sac chamber and the discharge hole of a D.I. diesel injection nozzle by using a transparent model nozzle”, SAE 972942, 1997

[16] Arcoumanis, C., Flora, H., Gavises, M., Kampanis, N. And Horrocks, R. ”Investigation of cavitation in a vertical multi-hole injector”, SAE Paper 1999-01-0524,1999.

[17] Ganippa, L.C., Bark, G., Andersson S. and Chomiak J. ”The structure of cavitation and its effect on the spray pattern in a single-hole diesel nozzle. SAE Paper 2001-01-2008.

[18] Walther, J., Schaller, J.K., Wirth, R. and Tropea, C., "Characterization of cavitating flow fields in transparent diesel injection nozzles using fluorescent particle image velocimetry", ILASS-Europé, Darmstadt, September 2000.

[19] Baddock, C., Wirth, R., Fath, A., and Leipertz, A., ”Application of laser light sheet technique for the investigation of cavitation phenomena in real size diesel injection nozzles” ILASS – Manchester, pp. 236-241, July 1998.

[20] Baddock, C., et al. 1997 ”Fundamental study of the influence of cavitation on the internal flow and atomization of diesel sprays”. In: Proceedings of ILASS –97, Florence, Italy, pp. 53-59.

[21] Chaves, H., Knapp, M., Kubitzek, A., Obermeier, F., and Schneider, T., ”Experimental study of cavitation in the nozzle hole of diesel injectors using transparent nozzles”, SAE 950290, 1995.

[22] Baddock, C., Wirth, R., Fath, A., and Leipertz, A.,”Investigation of cavitation in real size diesel injection nozzles” International journal of heat and fluid flow, Elsevier, Vol. 20, pp. 538-544, 1999.

[23] Prescher K. and Schaffitz W., ”Verschleiss von Kraftstoff-Einspritzdüsen für Dieselmotoren infolge Kraftstoffkavitation,” MTZ Motortechnische Zeitschrift, 40, 173-178, 1979.

[24] Gooney, K.H. and Corradini, M.L., ”Isolated effects of ambient pressure, nozzle cavitation and hole inlet geometry on diesel injection spray characteristics”, SAE Paper 2000-01-2043, 2000.

[25] Nurick, W.H., ”Orifice cavitation and its effect on spray mixing”. Journal of Fluids Engineering, Vol. 98, pp. 681-687, 1976.

[26] Ohrn, T.R., Sensor, D.W:, and Lefebvre, A.H., ”Geometrical effects on discharge coefficient for plain-orifice atomizers”, Atomization and sprays, Vol. 1, No. 2, pp. 137-153, 1991.

[27] Sirignano, W.A. and Mehring, C. (2000) “Review of theory of distortion and disintegration of liquid streams”. Progress in energy and Combustion Science, 26, 609-655.

[28] Arcoumanis, C. and Gavises, M., ”Linking nozzle flow with spray characteristics in a diesel fuel injecion system,” Atomization and sprays, Vol. 8, pp. 307-347, 1998.

[29] Soteriou, C., Andrews, R. and Smith, M., ”Direct injection diesel sprays and the effect of cavitation and hydraulic flip on atomization”, SAE Paper 950080

[30] Heimgärtner, C., Leipertz, A. “Investigation of the Primary Spray Breakup Close to the Nozzle of a Common – Rail High Pressure Diesel Injection System, SAE 2000-01-1799.

[31] Fluid Mechanics with Engineering Application, R.L. Daugherty et al., Mc Graw Hill, 1989.

[32] Dumont et al. 2000, ”Cavitating flow in diesel injectors and atomization – a bibliographical review”, Eighth international conference on liquid atomization and a spray systems, Pasadena, USA.

[33] Kent, J.C. and Brown, G.M. (1983) Nozzle exit flow characteristics for square-edge and rounded inlet geometries. Combustion Science Technology, 30, 121-132.

[34] Reitz R. D. and Bracco F. B., ”On the dependence of spray angle and other spray parameters on nozzle design and operating conditions,” SAE Paper 790494, 1979.

[35] Winklehofer, E. ”Velocities and structure of atomizing diesel sprays” ILASS – Europé, Florence –97

[36] Han, J., ” Investigation of Diesel Spray Primary Break-up and Development for Different Nozzle Geometries”. SAE 2002-01-2775

[37] Siebers D.L., ”Liquid-phase fuel penetration in diesel sprays” SAE Paper 980809

[38] Hiroyasu, H. and Arai, M. ”Structures of fuel sprays in diesel engines” SAE Paper 900475

[39] Kamimoto, T. et al., ”Effect of high pressure injection on soot formation processes in a rapid compression machine to simulate diesel flames” SAE Paper 871610

[40] Gooney, K.H. and Corradini, M.L., ”Isolated effects of ambient pressure, nozzle cavitation and hole inlet geometry on diesel injection spray characteristics”, SAE Paper 2000-01-2043, 2000.

[41] Koo, J., “Influence of Fuel Injector Nozzle Geometry on Internal and External Flow Characteristics” SAE 970354

[42] Tamaki, T. et al., ”Effect of cavitating and internal flow on atomization of a liquid jet”, Atomization and Sprays, Vol. 8, No. 2, pp. 179-197, 1998.

[43] Kampmann, B. et al. “The influence of hydro grinding at VCO nozzles on the mixture preparation in a DI Diesel engine”, SAE 960867.

[44] Su, T. and Farell, P., “Nozzle effect on high pressure diesel injection” SAE 950083

[45] Su, T. and Farell, P., “Characterization of high injection pressure diesel sprays with relation to particulate and NOx emissions”. Atomization and Sprays, vol. 8 pp. 83-107, 1998.

[46] Heimgärtner, C. and Leipertz, A. “Investigation of the primary spray breakup close to the nozzle of a common rail high pressure diesel injection system. SAE 2000-01-1799.

[47] Chomiak, J. and Karlsson, J.A.J., 1996: Flame liftoff in diesel sprays, 26th Symposium (International) on Combustion, The Combustion Institute, Pittsburgh, PA, 2557-2564.

[48] Dec, J.E., 1997: A Conceptual Model of DI Diesel Combustion Based on Laser-Sheet Imaging, SAE paper 970873.

[49] Flynn, P. F. et al., 1999: Diesel Combustion: An Investigated View Combining Laser Diagnostics, Chemical Kinetics, and Empirical Validation, SAE paper 1999-01-0509.

[50] Naber, J. and Siebers D.L., ”Effects of gas density and vaporization on penetration and dispersion of Diesel sprays” SAE Paper 960034

[51] Siebers D.L. and Higgins, B., “Flame lift-off on direct-injection Diesel sprays under quiescent conditions”. SAE 2001-01-0530

[52] Pickett, L. and Siebers, D. “Effect of orifice diameter on the structure of Diesel spray flames”, Combustion Institute, Oakland, CA, March 2001.

[53] Kamimoto, T. et al. “High combustion temperature for the reduction of particulate in Diesel engines” SAE 880423.

[54] Smith, O.I., 1981: Fundamentals of Soot Formation in Flames with Application to Diesel Engine Particulate Emissions, Progress in Energy and Combustion Science, 7:275-291.

[55] Bockhorn, H.(eds.): Soot formation in Combustion: Mechanisms and Models. Springer-Verlag, Berlin Heidelberg (1994).

[56] Glassman, I., 1996: Combustion, 3rd edition. Academic Press, Inc., San Diego.

[57] Moh'd Abu-Qudais; Andreas Matson; David Kittelson “Combination of methods for characterization diesel engine exhaust particulate emissions” JSME International Journal, Series B: Fluids and Thermal Engineering. 2001;44(1):166-170.

[58] Higgins B., Siebers D.L. "Measurement of the flame lift-off location on DI Diesel sprays using OH chemiluminescence” SAE Paper 2001-01-0918.

[59] Pickett, L. et al. ”Relationship Between Ignition Processes and the Lift-Off Length of Diesel Fuel Jets” SAE 2005-01-3843

[60] Johnson, J. et al. “Investigation of Diesel liquid spray penetration fluctuations under vaporizing conditions”. SAE 2012-01-0455.

[61] Karasawa T. et al. ” Effect of nozzle configuration on the atomization of a steady spray” Atomization and sprays, vol. 2, pp. 411-426 (1992).

[62] Koo, J. et al. “Influence of Fuel Injector Nozzle Geometry on Internal and External Flow Characteristics” SAE 970354.

[63] Matsui, Y. “A Study on the Time and Space Resolved Measurement of Flame Temperature and Soot Concentration in a D. I. Diesel Engine by the Two-Color Method” SAE 790491

[64] Musculus, M. and Kattke, K. “Entrainment waves in Diesel jets” SAE 2009-01-1355

[65] Musculus, M. et al. “End-of-Injection Over-Mixing and Unburned Hydrocarbon Emissions in Low-Temperature-Combustion Diesel Engines” SAE 2007-01-0907

[66] Musculus, M. “Effects of the in-cylinder environment on diffusion flame lift-off in a DI Diesel engine” SAE 2003-01-0074.

[67] Siebers et al. “Flame Lift-Off on Direct-Injection Diesel Fuel Jets: Oxygen Concentration Effects” SAE 2002-01-0890

[68] Siebers, D. and Higgins, B. “Effects of injector conditions on the flame lift-off length of DI Diesel sprays”. SAND2000-8249 (2000).

[69] Dec, J. et al. “Diffusion-flame/wall interactions in a heavy-duty DI Diesel engine” SAE 2001-01-1295.

[70] Kittelson, D. et al. “Particulate emissions from Diesel engines – influence of in-cylinder surface” SAE Transactions, Vol. 99, Sec. 3, paper no. 900645, 1990.

[71] Dahlen, L. “On applied CFD and model development in combustion systems development for DI Diesel engines: Prediction of soot mediated oil thickening” Doctoral Thesis, Internal combustion engines, Royal institute of technology, Stockholm 2002.

[72] Borthwick, P. and Farrell, P. “Fuel injection spray and combustion chamber wall impingement in large bore diesel engines” SAE 2002-01-0496.

[73] Fath, A. et al. “Spray break-up process of Diesel fuel investigated close to the nozzle”, ICLASS-97, August 18-22, 1997, Seoul.

[74] Badock, C. et al. “ The influence of hydro grinding on cavitation inside a Diesel injection nozzle and primary break-up under unsteady pressure conditions”. ILASS Europe 99, Toulouse 5-7 July 1999.

[75] Winklhofer, E. et al. “Basic flow process in high pressure fuel injection equipment”. ILASS Europe 2003, Sorrento, Italy 13-17 July.

[75] Larsson, A. “Optical studies in a Diesel engine” SAE 1999-01-3650.

[76] Schwarz, V. et al. “Analysis of Mixture Formation, Combustion and Pollutant Formation in HD Diesel Engines using Modern Optical Diagnostics and Numerical Simulation” SAE 1999-01-3647.

[77] Blessing, M. et al. “Analysis of Flow and Cavitation Phenomena in Diesel Injection Nozzles and Its Effects on Spray and Mixture Formation” SAE 2003-01-1358.

[78] Pierpoint, D. and Reitz, R. “Effect of injection pressure and nozzle geometry on D.I. Diesel emissions and performance” SAE 950604.

[79] Payri, F. et al. “The influence of cavitation on the internal flow and the spray characteristics in diesel injection nozzles” Elsevier, Fuel 83, p.419-431 (2004).

[80] Desantes, J.M. et al. “Influence of cavitation phenomenon on primary break-up and spray behavior at stationary conditions.” Elsevier, Fuel 89, p.3033-3041 (2010).

[81] Ho, C., and Gutmark, E., “Vortex induction and mass entrainment in a small-aspect-ratio elliptic jet”, J.Fluid Mech., Vol. 208, pp 382-405, 1987.

[82] Hussain, F., and Husain, H.S., “Elliptic jets. Part 1, Characteristics of unexcited and excited jets”, Fluid Mech., Vol. 208, pp 257-320, 1989.

[83] Xi, D.G., Yang, Y.X., Zhang, J.B., and Shi, S.X., “Experimental study on spray from nozzles of elliptic orifice”, AMD-Vol.151/PVP-Vol.247, Symposium on Flow-Induced Vibration and Noise, ASME, vol.7, 1992.

[84] Yamamoto, H., and Niimura, K., “Characteristics of Fuel Sprays from Specially Shaped and Impinging Flow Nozzels”, SAE Paper 950082.

[85] Gong, Y., Changwen, L., Yezhou, H., Zhijun, P., “An Experimental Study on Droplet Size Characteristics and Air Entrainment of Elliptic Sprays”, SAE Paper 982546.

[86] Jacobsson, L., and Chomiak J., “Injection Orifice Shape: Effects on Combustion and Emission Formation in Diesel Engines”, Transactions of the SAE, Vol. 106, Sect. 4, pp. 1479-1496, SAE Paper 972964, 1997.

[87] Jacobsson, L., Winklhofer, E., and Chomiak J., “Injection Orifice Shape: Effects on Spray Characteristics and Heat-Release Rate in a Large-Size Single-Cylinder Diesel Engine”, SAE Paper 1999-01-3490.

[88] Schmid, M. et al. “Influence of nozzle hole geometry, rail pressure and pre-injection on injection, vaporisation and combustion in a single-cylinder transparent passenger car common rail engine”, SAE 2002-01-2665.

[89] Charlton, S., Heavy duty Diesel emission control symposium, presentation, Gothenburg Sweden 2007.

[90] Pipho, M. et al. “Injection timing and bowl configuration effects on in-cylinder particle mass”, SAE 921646.

[91] Zhao, H. et al. “Time-resolved measurements and analysis of in-cylinder gases and particulates in compression-ignition engines”, SAE 961168.

[92] Ganippa, L. et al. “Transient measurements of discharge coefficients of Diesel nozzles”, SAE 2000-01-2788.